Icarus **141**, 367–387 (1999)
Article ID icar.1999.6166, available online at http://www.idealibrary.com on IDEAL®

Large Scattered Planetesimals and the Excitation of the Small Body Belts

Jean-Marc Petit, Alessandro Morbidelli

Centre National de la Recherche Scientifique, Observatoire de Nice, B.P. 4229, 06304 Nice Cedex 4, France

and

Giovanni B. Valsecchi

IAS—Planetologia, Area di Ricerca del C.N.R., Via Fosso del Cavaliere, 00133 Rome, Italy

Received May 15, 1998; revised May 3, 1999

We study the dynamical excitation that large planetesimals, scattered either by Neptune or Jupiter, could have provided to the primordial Edgeworth–Kuiper belt and the asteroid belt. Using both a refined Monte Carlo approach and direct numerical integration, we show that the Monte Carlo method is useful only to give qualitative insight into the resulting excitation, but cannot be trusted from a quantitative viewpoint. According to our direct integrations, Neptune-scattered planetesimals of mass from a few tenths to one Earth mass could have ejected most of the bodies from the primordial Edgeworth–Kuiper belt, thus explaining the large mass deficiency of the present belt up to about 50 AU. The remaining bodies are left on orbits with eccentricity and inclination comparable to those observed. This dynamical excitation is not restricted to the inner part of the belt but may extend to 100 AU. We also show that Pluto has too small a mass to destabilize the motion of other bodies in the 2 : 3 mean motion resonance with Neptune. The same mechanism involving Jupiter-scattered planetesimals of about one Earth mass can excite the outer asteroid belt, hence depleting it of most of its primordial mass. However, this fails to excite the inner belt. In the case where the planetesimals are isolated by mutual gravitational perturbations on long-lived main-belt-like orbits, safe from encounters with Jupiter, the resulting asteroid belt is very similar to the currently observed one, in terms of mass deficiency, excitation in eccentricity and inclination, and radial mixing. Pallas-like bodies are also obtained. However, the decoupling of planetesimals from Jupiter on well-behaved orbits is rather improbable (2% of our simulations), and the resulting asteroid belt is very critically dependent on the mass of the scattered planetesimals and their residence time in the belt. © 1999 Academic Press

Key Words: **asteroids; Kuiper belt objects; origin, solar system; planetesimals.**

I. INTRODUCTION

The existence of the asteroid belt and of the Edgeworth–Kuiper belt, both dynamically excited (Fig. 1) and with a total mass that is only a small fraction of the original one, is very intriguing and may provide several clues for understanding the formation phase of our Solar System. The existence and the main properties of the belts of small bodies should be considered as observational constraints to discriminate among scenarios of Solar System's primordial evolution. The large number of bodies in the belts make them statistically significant sets of evidence.

Concerning the asteroid belt, restricting to the bodies larger than 50 km in diameter (the only ones that have a chance to be primordial, and whose distribution is not contaminated by the families), we can naturally distinguish three zones: the *inner belt* with $a < 2.5$ AU (3 : 1 mean motion resonance with Jupiter), the *central belt* with $2.5 < a < 3.28$ AU (2 : 1 resonance), and the *outer belt*, beyond 3.28 AU (Fig. 1a). In the outer belt, all asteroids beyond 3.8 AU are in mean motion resonances with Jupiter. The most striking aspects that one would like to explain with a unitary model are the following.

(i) Its strong dynamical excitation. The median eccentricity and inclination of the bodies larger than 50 km are: in the inner belt, 0.15 and 6°, respectively; in the central belt, 0.14 and 10.7°; and in the outer belt, 0.1 and 12.1°. In the outer belt, the median eccentricity is lower than in the other parts because of the instabilities due to Jupiter that tend to deplete the region above the solid line in Fig. 1a, with the exception of the bodies in the 3 : 2 and 4 : 3 resonances. Actually, the absence of bodies at low eccentricity and inclination ($e < 0.05$, $i < 2°$), a region stable over the age of the solar system (Duncan 1994; Holman and Murray 1996), indicates that the primordial excitation in the outer belt has been even larger than that in the rest of the asteroid belt, as confirmed by the larger median value of inclination. In the central belt, the existence of 2 Pallas on an orbit with $e = 0.23$ and $i = 34.8°$ is by itself a challenge which has not been sucessfully overcome, up to now.

(ii) Its large mass depletion. The present total mass of the asteroid belt is estimated to be of order 5×10^{-4} $M_\oplus$ ($M_\oplus =$ Earth mass), 10^2–10^3 times smaller than its primordial mass

0019-1035/99 $30.00

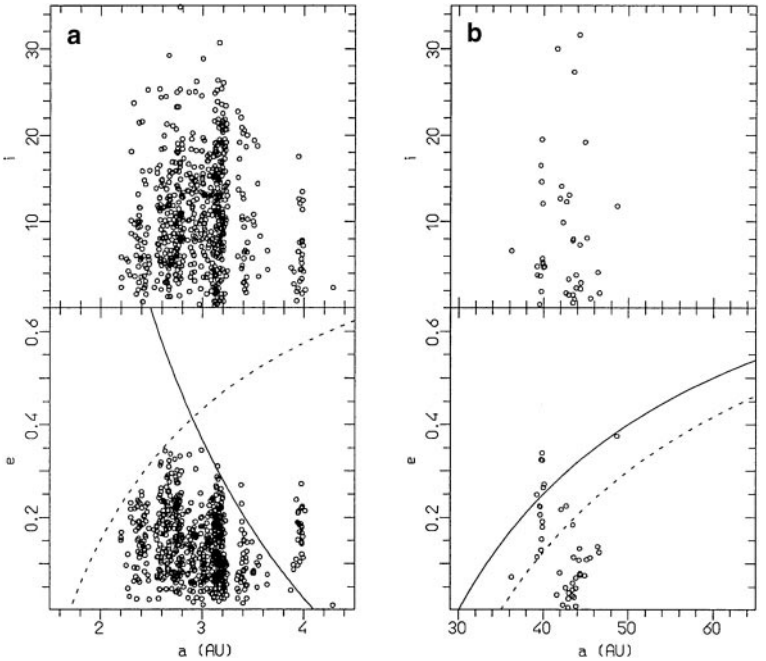

FIG. 1. Osculating inclination (top) and eccentricity (bottom) versus semimajor axis for the asteroid belt (a) for bodies larger than 50 km in diameter (solid line: aphelion distance at 4.1 AU; dashed line: perihelion distance at 1.7 AU) and for the Edgeworth–Kuiper belt with multiopposition orbits at December 15, 1998 (b) (solid line: perihelion distance at 30 AU; dashed line: perihelion distance at 35 AU).

(Weidenschilling 1977). The accretion of the largest asteroids on a timescale comparable with the meteoritic solidification age also implies the primordial existence of at least 100 times more material than at present (Wetherill 1989). This shows that the important mass deficiency of the asteroid belt is not due to the presence of a gap in the primordial disk, but is the result of some process which occurred after the asteroids' formation. From Fig. 1a, we see that the mass deficiency is larger in the inner and outer belts than in the central part.

(iii) The radial mixing of asteroid types. The optical properties of the asteroids depend roughly on their distance from the Sun: S-types dominate the inner belt, C-types are the most abundant in the central belt, while P-types dominate in the outer belt, with the exception of the Trojan population, which is mainly of D-type. This radial compositional zoning likely reflects the temperature gradient of the primitive nebula. However, the boundaries between compositional zones are not sharp: asteroids of different types are mixed over scales $\sim$1 AU (Gradie and Tedesco 1982). Such mixing is not easily explained by the turbulence of the primitive nebula or by the radial decay of pristine bodies due to gas drag (Ruzmaikina *et al.* 1989).

The structure of the Edgeworth–Kuiper belt (EK belt or EKB hereafter) is in many aspects similar to that of the asteroid belt (see Morbidelli 1998 for a review). The belt is dynamically excited and appears to have a sharp transition at the 40- to 42-AU boundary, allowing a natural distinction between an *inner belt* ($a < 40$ AU) and the *classical belt* ($a > 41$ AU, and perihelion distance $q > 35$ AU, the latter being the limit of stability if not in mean motion resonance with Neptune). The $\sim$40–42 AU region is dynamically unstable due to the presence of secular resonances (Knežević *et al.* 1991; Duncan *et al.* 1995; Morbidelli *et al.* 1995). In the inner belt the orbital excitation is very high. The dynamically stable region with $e < 0.05$ between 36 and 40 AU (Duncan *et al.* 1995) appears to be depleted of objects; all the transneptunian bodies discovered with $a < 40$ AU have larger eccentricities, and therefore are in some mean motion resonance with Neptune, since the latter are the only stable regions available if the perihelion distance is smaller than $\sim$35 AU. The bodies in the 2 : 3 resonance ($a \sim 39.54$ AU) have eccentricities ranging from 0.1 to 0.35; the inclinations are also quite excited, with a median value of 5.1°. In the classical belt the orbital excitation is smaller but still notable, with median eccentricity and inclination equal to $\sim$0.07 and $\sim$4.0° respectively. Although these numbers do not account for observational biases (see Section III), they show that the classical belt is dynamically excited. The total mass of the belt in the 30–50 AU zone is estimated to be between 0.12 and 0.26 $M_\oplus$ (Jewitt *et al.* 1998), much smaller than its primoridal value of $\sim$30 $M_\oplus$, which can be computed by extrapolating the distribution of solid material in the outer planetary region, using a power law with a slope of -2 versus heliocentric distance (Weissman and Levison 1996). Stern 1996 showed that to grow objects as big as 100 km within a time not exceeding the Solar System age, the mass of the belt between 35 and 50 AU had to be equal to several Earth masses. More precisely, 4 $M_\oplus$ are required if the primordial belt was an extremely cold disk ($e = 0.001$), while 30 $M_\oplus$ are required in a more realistic case ($e = 0.01$). A more recent accretion model

by Kenyon and Luu (1998) gives similar results. Therefore, as in the asteroid belt case, the EKB shows a large mass depletion which must be the result of processes which occurred after the accretion of the transneptunian objects. Finally, recent observations tend to show the existence of two spectroscopically distinct populations which are apparently radially mixed (Tegler and Romanishin 1998). But this is a controversial result (Barucci *et al.* 1998).

To explain the large mass deficiencies of the asteroid and of the EK belts, intense primordial collisional activities have been invoked. Because large bodies cannot be collisionally destroyed, the collisions could have reduced the total mass to a few percent only if the original number of large bodies was basically the same as the present one and the original size distribution was very steep (see Davis *et al.* 1979 or Wetherill 1989 for the asteroid belt; Stern and Colwell 1997 or Davis and Farinella 1998 for the EKB). However, in the asteroid belt the survival of the fragile basaltic crust of Vesta is an important argument against primordial collisional activity significantly more important than at present (Davis *et al.* 1994); in the EKB, "the large tilts of Uranus and Neptune, the capture of Triton and the formation of the Pluto–Charon binary each argue for the past presence of numerous 1000 km bodies in the 20–50 AU region" (Stern 1991). Therefore it seems that the large mass deficiencies of the small-body belts also require dynamical mechanisms capable of displacing most of the material into the unstable regions.

The scenarios that have been proposed to explain the orbital excitation of the small bodies of the Solar System can be classified in two categories: those which invoke the sweeping of the belts by resonances of various type, and those which invoke the scattering action of massive planetesimals which have later been ejected from the Solar System by planetary perturbations.

The idea that secular resonances could have swept the asteroid belt as a result of the dissipation of the primordial nebula was first proposed by Ward *et al.* (1976). Ward (1980) and Heppenheimer (1980) developed a planar analytic linear model which showed that the current eccentricities of the asteroids could be explained by the passage of two secular resonances through the asteroid belt. However, the numbers of objects ejected into the unstable regions would have been very limited. Lemaitre and Dubru (1991) developed a nonlinear model and found smaller eccentricity excitation than in the previous works. Moreover they also investigated the possibility that secular resonances excited the asteroidal inclinations, with no encouraging results. Lecar and Franklin (1997) made numerical simulations of secular resonance sweeping in a planar model of the asteroid belt, including gas drag, and found a strong depletion of the outer belt and a general eccentricity excitation—but few ejections—in the inner and central belts. Gomes (1997) investigated the effects of the migration of secular resonances forced by the radial migration of Jupiter and Saturn, finding again a general eccentricity excitation, but no inclination excitation beyond 2.7 AU. Liou and Malhotra (1997) investigated the effects of the migration of mean motion resonances forced by the radial migration of Jupiter, finding a potential mechanism for the depletion of the outer asteroid belt but no significant effect on the inner and central belts.

If these models were successful in explaining all the main features of the asteroid belt, they would provide information on the mass of the solar nebula and its dissipation time scale and/or the radial migration of Jupiter and Saturn. However, none of these models succeeds in explaining all the features at once. If the free parameters are adjusted to reproduce the observed eccentricity distribution of the asteroids, then the fraction of bodies ejected into the planet-crossing region turns out to be too small to explain the mass depletion of the belt. Moreover, the inclination is not efficiently excited throughout the belt. Objects on orbits such as that of Pallas are not obtained. Last, but not least, the radial mixing of taxonomic types is not reproduced, because basically the objects conserve their primordial semimajor axes.

Concerning the EKB, the Malhotra (1995) model of sweeping mean motion resonances sucessfully explains the existence of several objects in the $2:3$ resonance with Neptune, their distribution in eccentricity and inclination, and the depletion of the stable nonresonant region between 36 and 39 AU and with eccentricity smaller than 0.05. This is obtained by an outward smooth migration of Neptune by 7–8 AU. However, it does not explain the dynamical excitation of the population observed beyond 42 AU nor the strong mass depletion. The effects of the outward migration of the ν_8 secular resonance have been studied by Levison *et al.* (1997b) but resulted in an eccentricity excitation that is too small for $a < 40$ AU and almost zero beyond 42 AU, in disagreement with the observations.

The idea that large Jupiter-scattered planetesimals (LJSPs) of mass comparable to that of Earth could have dynamically heated the asteroid belt was first proposed by Safronov (1979). The existence of large planetesimals as leftover of planetary formation is predicted by all the current planetary formation theories. The tilts of the spin axes of Saturn, Uranus, and Neptune support the idea of collisions with massive bodies (about the mass of the Earth). A number of works have quantitatively explored the effects of LJSPs on the asteroid belt in the goal of explaining its present structure and providing a constraint on the number, mass, and lifetime of these planetesimals. Davis *et al.* (1979) estimated, using a gas-like model, that five one-Earth-mass LJSPs, crossing the belt over 3 Myr, could provide the required eccentricities. Ip (1987) was the first to attempt to follow the dynamical evolution of LJSPs and asteroids. For this purpose, he used a Monte Carlo code based on the method of Arnold (1965) to account for the statistical effects of close encounters, but neglected distant perturbations and resonant phenomena, as well as the mutual encounters among the LJSPs. He found that the LJSPs have dynamical lifetimes that are too short for them to be efficient asteroidal perturbers; only if Jupiter were smaller, $1/10$ of its present mass, for $\sim$10 Myr could the LJSPs' action be more important. In particular, 50 LJSPs, each of mass 3×10^{27} g, could excite the asteroid belt in this scenario. Wetherill (1989), also using Monte Carlo simulations but

including the mutual encounters among LJSPs, contradicted the conclusions of Ip. He found that, even in the case of a full-sized Jupiter, a LJSP might decrease its eccentricity due to an encounter with another LJSP, isolating itself in the asteroid belt, safe from Jupiter's encounters. The isolated body would then have a sufficiently long lifetime to excite the asteroid belt by gravitational scattering. In this scenario, only 10% of the asteroids would survive more than 700 Myr, with a distribution of eccentricities and inclinations similar to the observed one. Moreover the gravitational scattering would also provide an important mixing in the radial distribution of asteroidal compositional types.

Wetherill (1992) alternatively proposed that the asteroid belt was originally a massive dynamically cold system, which contained about 200 sublunar- to martian-sized planetesimals within its population. These planetesimals excited each other by mutual interactions until they all fell under the gravitational influence of Jupiter and were ejected from the Solar System. At the end of this phase, only a small fraction of the original asteroids survived in the stable regions of the belt, on eccentric and inclined orbits. The Monte Carlo simulations, including also a rough model of resonant dynamics, made this scenario quantitatively appealing. Nevertheless, some concern remained common in the community about the possibility that *all* large-sized planetesimals would leave the asteroid belt. Therefore Wetherill and Chambers (1997) and Chambers and Wetherill (1998) simulated the dynamical evolution of 40 martian-sized planetesimals in the asteroid belt with an N-body integrator, confirming that the quasi-simultaneous ejection of all the planetesimals is dynamicaly plausible.

The idea that large Neptune-scattered planetesimals (LNSPs) could be responsible for the currently observed structure of the EKB was proposed by Morbidelli and Valsecchi (1997). The evolution of 100 test LNSPs was simulated using an accurate numerical integrator and their effects on the transneptunian objects of the EKB were estimated using Öpik formulae (Öpik 1976). The computations showed that the EKB could be easily excited as far as 60 AU, provided that a few planetesimals of mass $\sim 2\ M_\oplus$ are scattered by Neptune. As a result of the excitation, in the inner EKB the only surving transneptunian bodies (a few percent of the initial population) would be in mean motion resonances with Neptune.

In the present paper we intend to simulate using modern tools the effects that large planetesimals scattered by Neptune or by Jupiter would have on the EK belt or on the asteroid belt, respectively. We first estimate the minimal effects those planetesimals would have, in a way similar to that of Morbidelli and Valsecchi (1997), but with a more detailed computation of the scattering effects. In the second stage, having obtained knowledge of what kind of initial conditions may give some interesting effects, we perform direct numerical simulations of the interesting cases. This two-stage approach allows us to drastically reduce the computing time by limiting the number of direct numerical simulations.

In the next section we will describe our numerical procedures for (i) simulating the dynamical evolution of the scattered planetesimals, (ii) computing the impulse velocities received by the small bodies due to their closest encounter with the planetesimals in the initially dynamically cold belts and relating this to the eccentricity and inclination excitations, and (iii) simulating directly the evolution of a set of test particles gravitationaly influenced by a giant proto-planet and planetesimals. Section III will discuss in detail the results concerning the EKB. We improve the results of Morbidelli and Valsecchi (1997), requiring a smaller number of LNSPs and smaller masses, and achieving a final orbital distribution which is more similar to the observed one, in particular regarding the excitation and the depletion of the belt beyond 42 AU. Integrating a set of full three-body problems (Sun–Neptune–massive planetesimal), we also check that the final orbital elements of Neptune are not incompatible with its present ones. We also show that as long as large planetesimals are present in the system, the orbital migration of Neptune is not an efficient mechanism for capturing EKB objects in mean motion resonances. In Section IV we will discuss the action of LJSPs on the asteroid belt, in the model where Jupiter is full-sized and in the model where its core is slowly growing from 5 to 15 $M_\oplus$ in 10 Myr. We will show that, conversely to what has been previously simulated with Monte Carlo codes, the LJSPs cannot be responsible for the sculpting of the asteroid belt. We then explore Wetherill's scenario (1989) of mutually interacting LJSPs and find that it could be efficient in exciting the asteroid belt, but this scenario has a low probability of occuring. Finally in Section V, we discuss the implications of these results and draw some conclusions.

To fix the notations, throughout the paper we will denote by "planetesimals" the massive bodies—usually scattered by the protoplanets—and by "small bodies" or "particles" the members of negligible mass of the asteroid and EK belts.

II. NUMERICAL PROCEDURES

In this section, we present the numerical methods used in this study. With our current computational resources, it is very time-consuming to integrate the complete equations of motion of hundreds to thousands of small bodies perturbed by large planetesimals, themselves scattered by a large protoplanet. Direct numerical integrations will not be used to explore the whole range of possible initial conditions. More efficiently, they will be used to quantify the effect of especially interesting cases that will be identified by a Monte Carlo approach (the latter giving a qualitative insight into the effects, but failing to give quantitative predictions). The Monte Carlo method works as follows. Integrating in the framework of the restricted three-body problem a large number of test particles, we create a database on the statistical dynamical evolution of the scattered planetesimals. Next we use these statistics to estimate the effect that the scattered planetesimals would have, by gravitational interaction, on the small bodies of the asteroid or of the EK belts, in terms of

random velocity excitation, and relate the latter to the variation in eccentricity and inclination.

For the direct simulation of the interesting cases, we use a version of the SWIFT code (Levison and Duncan 1994) that we have modified to integrate the evolution of a set of test particles with the protoplanet and planetesimals following given evolutions.

II.A. Generating a Database of Orbital Evolution

We first integrate the equations of motion of the restricted three-body problem. The two massive bodies are the Sun and either a proto-Jupiter or a proto-Neptune. The orbit of the protoplanet is fixed. The motion of a massless test particle relative to the Sun is then integrated. We have not taken into account any other planet because we know that the primordial planetary system was probably somewhat different from the present one and we want to be sure that our results are not strongly dependent on some specific secular resonance, the location of which could have been different in the primordial system. Therefore, we have chosen on purpose the simplest dynamical model, believing that it is also the most generic one. Depending whether we are constructing an orbital database for LJSPs or LNSPs we have different initial and stopping conditions.

We present first the LNSP initial conditions. Two sets of integrations have been performed, with the mass of Neptune chosen to be the present one. Neptune's orbital elements are the present ones, except that the inclination is taken to be zero; because we consider a fixed ellipse for Neptune's orbit, this corresponds to simply change the reference plane. For the first set of integrations, we have considered 100 test planetesimals with the following randomly chosen initial conditions: semimajor axis $a \in [32, 34]$ AU (uniformly distributed in $1/a$), perihelion distance $q \in [30.5, 31.5]$ AU, and inclination $i \in [0, 1.5]^\circ$. The three angles ω, Ω, and f are drawn randomly in the range $[0, 360]^\circ$. We call these the internal LNSPs (set I). In the second set, we choose at random 100 test planetesimals with larger semimajor axis $a \in [34, 36]$ AU, everything else being the same as before. We call these the external LNSPs (set II). The reason for choosing two sets of planetesimals was to understand the influence of the initial conditions on the final excitation of the EKB. Choosing a planetesimal's semimajor axis up to 36 AU is legitimate since we know from Duncan *et al.* 1995 that the region up to 36 AU is dynamically rapidly unstable. All bodies must suffer an increase of eccentricity until their perihelion is decreased to less than 31.5 AU where the first strongly scattering encounters with Neptune takes place (Duncan *et al.* 1995). Our initial conditions aim at reproducing the beginning of this scattering phase. Note that with these initial conditions, all the test planetesimals have aphelion distance smaller than 37.5 AU for set I and 41.5 AU for set II; therefore, only those which undergo Neptune's scattering action can penetrate the classical EKB ($a > 42$ AU).

Each integration was stopped whenever the test planetesimal either came to a perihelion distance smaller than 20 AU (where the gravitational interactions with Uranus would become dominant) or was ejected on a hyperbolic orbit. If neither of these conditions occurred, the simulation was stopped after 100 Myr of integration time (14 out of 100 internal test planetesimals survived 100 Myr, and 24 out of 100 external ones).

In the case of the LJSPs, we performed two sets of integrations. In the first set (set III), we used the present mass, semimajor axis, and eccentricity for Jupiter. Again, its inclination was set to zero. We considered 100 planetesimals with a fixed eccentricity of 0.01, a semimajor axis regularly distributed in the range [4.0, 4.8] AU, and a randomly chosen inclination $i \in [0, 1]^\circ$. The other three angles were also randomly chosen, in the range $[0, 360]^\circ$. The choice of the semimajor axis range covers the regions which are dynamically unstable on a short time scale due to Jupiter's perturbations (Wisdom 1980; Duncan 1994). Each integration was stopped whenever the test planetesimal reached a heliocentric distance larger than 20 AU, from which it is very unlikely that they would ever come back to the inner solar system. If this condition did not occur, the simulation was stopped after 1 Myr of integration time (15 out of 100 test planetesimals survived 1 Myr staying on low eccentricity orbits which never encountered Jupiter).

In set IV, the mass of Jupiter grows linearly with time from 5 to 15 $M_\oplus$ over 10 Myr. Jupiter's semimajor axis and eccentricity are the present ones, and the inclination was set to 0. The planetesimals have the same orbital elements as in set III, except for the semimajor axis, taken in the range [4.62, 5.1] AU. This roughly corresponds to the range of unstable orbits for the considered range of Jupiter's mass (Wisdom 1980). Again, each integration was stopped whenever the test planetesimal reached a heliocentric distance larger than 20 AU or after 10 Myr (only two planetesimals were ejected during that time). After 10 Myr, Jupiter should accrete the surrounding gas very rapidly and reach its present mass of more than 300 $M_\oplus$ in a very short time (Pollack *et al.* 1996). After this event, the following evolution would be statistically equivalent to that of set III.

In our databases of orbital evolutions, we kept record of each orbit, in term of the six orbital elements at each pericenter passage. This database is used both for the Monte Carlo estimates and for the direct simulations of the excitation of the small body belts. In the Monte Carlo treatment, a planetesimal orbit will be assumed to be fixed with the specified orbital elements for the next revolution. In the direct simulations, the planetesimal orbit is linearly interpolated at each time step. In this way, we reduce the amount of storage needed, while storing at each orbital revolution ensures that the changes are not too large from one record to the other.

II.B. Deviation of Small Body Orbits

We now try to estimate the minimal gravitational effect of the planetesimals when they cross the primordial belts of small bodies. We consider an annulus of mean semimajor axis a, width Δa, and height $2a \sin(i_{\max})$ (in all the simulations presented here, we fix $i_{\max} = 1^\circ$). For this annulus, we compute (i) the

mean encounter speed between a small body (with orbital radius a, $e=0$, $i=0$) and the planetesimal, (ii) the total number of crossings of that annulus by all the planetesimals, and (iii) the mean length of the arc of the planetesimal's orbit that intersects the annulus, computed in the frame corotating with the annulus. The later quantity will be used to estimate the typical impact parameter for an encounter.

Let a_p, e_p, and i_p be the semimajor axis, eccentricity, and inclination of the planetesimal, which intersect the planar–circular orbit of the particle. We check if the planetesimal intersect the annulus defined above. If it does, then we compute the relative velocity of the two bodies at the intersection point, scaled by the velocity on the circular orbit (Öpik 1976; Valsecchi and Manara 1997),

$$U = \sqrt{3 - T}, \tag{1}$$

where T is the Tisserand parameter of the planetesimal with respect to the particle. We also compute the length of the arc of orbit of the planetesimal intersecting the annulus in the frame corotating with the annulus.

Applying this algorithm to all the orbits recorded in our database of orbital evolutions, we get, for each annulus, the mean encounter velocity relative to the local circular velocity $\langle U \rangle$, the total number of crossings or encounters N_c, and the mean arc length $\langle \alpha \rangle$.

The deviation of the small body by the planetesimal is computed with an impulse approximation, i.e., as a two-body problem. This is the well-known Rutherford scattering, also referred to as the Öpik approximation. The magnitude of the variation of relative velocity is

$$\Delta U = \frac{2U}{\sqrt{1 + \frac{b^2 U^4}{M_p^2}}}, \tag{2}$$

where M_p is the mass of the planetesimal in Solar mass units and b the impact parameter, i.e., the minimal approach distance between the two bodies if they were not gravitationally interacting, normalized to the radius of the circular orbit a. Here we assume that M_p is much larger than the mass of the small body. Hence the variation of relative velocity must be interpreted as the variation of velocity of the small body (in a vectorial sense), the planetesimal's orbit being unchanged.

For each annulus, we assume that the relative velocity U used in formula (2) is the mean velocity $\langle U \rangle$ that is computed from the database of the planetesimal orbital evolutions. We compute b as being the largest normalized (scaled by a) distance of approach such that the probability of having an encounter with an impact parameter less than b after N_c' crossings is a given number P. This is done as follows. The volume of an annulus is $V_a = 2\pi a \times \Delta a \times 2a \sin(i_{\max})$. The volume of a cylinder of length α and radius b is $V_b = \alpha \times \pi b^2$. Any test particle within the volume V_b will have an impact parameter less than b. For one transit of the planetesimal, the probability for each particle to have an impact parameter larger than b is V_b/V_a. Hence, for N_c' transits of the planetesimal, the probability of having at least one encounter with impact parameter less than b is $P = 1 - (1 - V_b/V_a)^{N_c'}$. One then obtains b by inverting the previous formula. If the impact parameter exceeds the height of the annulus, e.g., if $b > \sin(i_{\max})$, we use the volume $V_b = \alpha \times b \times \pi a \sin(i_{\max})$ in the computation of b.

The impact parameter b is a function of the number of crossings N_c' and of the mean arc length α. For each annulus, the typical impact parameter b is obtained by replacing α by $\langle \alpha \rangle$ computed from the database, and converting from N_c to N_c' as follows. In the preliminary integrations, we used a set of N particles, yielding N_c total crossings of an annulus. In the applications, we consider N' planetesimals of mass M_p. The actual number of crossings will then be $N_c' = N_c N'/N$.

From eq. (2) we see that ΔU is a function of the probability P through b. In the following section, we will commonly use three different values for P: 0.9, 0.5, and 0.1. This means that 90%, 50%, or 10% of the small bodies have suffered at least one encounter with one of the planetesimals with an impact parameter less than b. During that encounter, the change in relative velocity has been at least the one given by (2).

Up to now, we have only computed the change in velocity due to a close approach by a planetesimal. We are actually interested in the changes of semimajor axis δa, eccentricity δe, and inclination δi of the small body. Computing these would require knowledge of the exact encounter geometry. Following the statistical approach we have followed so far, we resorted to a large set of numerical integrations of encounters to obtain the distributions of $\delta a/a$, δe, and δi with respect to ΔU. We integrated restricted three-body problems with the Sun, a planetesimal of mass M_p, semimajor axis a_p, eccentricity e_p, and inclination i_p typical of our database, and a massless small body initially on a planar circular orbit of radius a. We varied at random all the other parameters. In Table I, we give the ratios $\delta e(P)/\Delta U(P)$, $\delta i(P)/\Delta U(P)$, $\delta a(P)/(a\Delta U(P))$, and $\sqrt{(\delta e(P))^2 + \sin^2(\delta i(P))}/\Delta U(P)$ for $P = 10\%, 50\%,$ and 90%. We can see that ΔU typically underestimates the eccentricity excitation by up to 50%, while it overestimates the inclination by 20 to 30%. The statistical relationship $\Delta e \sim 2\Delta i$ has been already pointed out (Ida and Makino 1992).

We want to stress that this approach underestimates the real effects. First, we only evaluate the effect of the strongest

TABLE I
Orbital Element Variations Relative to ΔU for Different Probabilities of Excitation

P	$\frac{\delta e(P)}{\Delta U(P)}$	$\frac{\delta i(P)}{\Delta U(P)}$	$\frac{\delta a(P)}{a\Delta U(P)}$	$\frac{\sqrt{(\delta e(P))^2 + \sin^2(\delta i(P))}}{\Delta U(P)}$
10%	1.48	0.73	1.49	1.67
50%	1.48	0.82	1.45	1.74
90%	1.06	0.65	0.82	1.71

encounter, neglecting the cumulative effects of more distant encounters. Second, as will be seen later, the Monte Carlo approach entirely misses the intricate interplay between the scattering action of the planetesimals and the dynamics induced by the protoplanet. However, it is very useful to find the class of planetesimal orbital evolutions and masses that will result in a sizeable effect.

II.C. Direct Numerical Integrations

In order to quantify the effects of a given initial configuration of planetesimals, we must resort to direct numerical integration. In integrating the motion of planetesimals, we were concerned with multiple close approaches between the planetesimal and the protoplanet. Hence, we used either a Radau of order 15 (Everhart 1985) or a Bulirsh and Stoer integrator (Stoer and Bulirsh 1980). For integrating the large number of test particles required for the direct simulations, we need to use the SWIFT code (Levison and Duncan 1994), which is the only available code that is fast enough. However, a direct use of SWIFT with the same initial conditions for the protoplanet and the planetesimal would result in a completely different evolution for the planetesimal since the latter is highly chaotic. We modified the SWIFT code so that it reads the orbital elements of the planetesimal and the protoplanet from the orbital element database. At each time step, the position of the protoplanet and the planetesimal are computed by a linear interpolation of their orbital elements in the database and these positions are then used to compute the motion of the test particles. The algorithm used here ensures that both positions and velocities of the two massive bodies are continuous functions of time. We tested this method against the standard SWIFT integrator and the Bulirsh and Stoer integrator by simulating the time evolution of a set of 100 massless test particles under the gravitational effect of the Sun, a protoplanet (Jupiter), and a planetesimal of mass 1 $M_\oplus$ on a stable orbit. Starting with the same initial conditions, we used both the SWIFT code and the Bulirsch and Stoer integrator to compare the outcomes of the two simulations since the actual orbit of the planetesimal is stable and hence is reproduced in each of the integrations. Next, we recorded the integrated orbits of the protoplanet and the planetesimal, with one output every 10^3 or 10^4 years, and used them as input for the modified SWIFT method, the initial conditions for the test particles being the same. We studied the statistical properties of the time evolution of the three test particle populations in terms of decaying number of particles versus time, distribution of eccentricity, and inclination. We found no statistically significant difference between these populations.

With all the tools described above, we proceed as follows. For both Neptune and Jupiter, we first apply the Monte Carlo approach on the sets of initial conditions defined above (Section II.A). Next, we select what seem to be the most interesting cases and perform direct numerical integrations using the modified SWIFT code. In two cases with Jupiter, the planetesimal is on a stable orbit. We then use the standard SWIFT code.

III. NEPTUNE SCATTERED PLANETESIMALS

Figure 2a shows, for illustrative purposes, the minimal excitation (ΔU) of the Edgeworth–Kuiper belt due to $N' = 3$ inner planetesimals of mass $M_{\rm P} = 1.5\ M_\oplus$ evolving according to the database constructed on the test planetesimals of set I (Section II.A). Following the recipe described in the previous section, we derived the excitation received during one encounter by 10% (dash–dotted line), 50% (dashed line), and 90% (solid line) of the small bodies initially on coplanar circular orbits.

This figure could be compared to Fig. 2a from Morbidelli and Valsecchi (1997) since it is computed with the same set of orbital integrations, except for the shorter integration time (50 Myr) in their case. The main difference is the divergence they found around 35–36 AU. This was the artifact of a rather crude approximation: assuming most of the encounters would occur with a large b, they approximated the value of $2\sin(\gamma/2)$ by γ. They also assumed, as a first approximation, that the typical relative velocity would be of the order of the circular velocity. So they had $\delta a/a \sim \delta e \sim \delta i \sim \gamma$. In fact, for heliocentric distances smaller than 36 AU, the number of crossings was very large, since all test particles started there, and some of them stayed there for the whole integration time. Hence the typical value of b was small and γ large. In the present study, we account for large deviation angles by considering the correct value of ΔU (2). This correction avoids the divergence found by Morbidelli and Valsecchi.

Nevertheless, we still find a distribution with two components. From 37 AU and up, the excitation is rather small (but not negligible !) and slowly decreasing with semimajor axis. Below that threshold, there is a sudden increase with the orbital excitation of 90% of the particles exceeding 0.05–0.1. As pointed out in the Introduction, this bimodal excitation actually qualitatively resembles the observed distribution of orbital elements of the Edgeworth–Kuiper belt objects (EKBOs). However, the observed transition between the highly and the moderately excited parts is in reality around 40–41 AU rather than 37 AU. In our simulation, the transition is precisely at 37 AU because the initial aphelion of the test planetesimals was in the range [35, 37] AU. This leads to a large number of passages through the belt up to 37 AU. Only the few planetesimals scattered further than 37 AU, and not rapidly ejected from the system, contribute to the excitation beyond 37 AU.

Next, we used another set of test planetesimals, with aphelion distance up to 41 AU (set II). The result is displayed in Fig. 2b, again with three planetesimals of mass $M_{\rm p} = 1.5\ M_\oplus$, and compares more satisfactorily with the known EKB distribution. The transition is now around 40 AU as observed. At the location of the 2 : 3 mean-motion resonance with Neptune (39.5 AU), the velocity excitation is in the range from 0.1 to 0.25; i.e., 90% of the particles would have an excitation larger than 0.1, and 10% an excitation larger than 0.25. This is in good agreement with the excitation in eccentricity and inclination of the observed objects in the 2 : 3 resonance. The large excitation would also explain

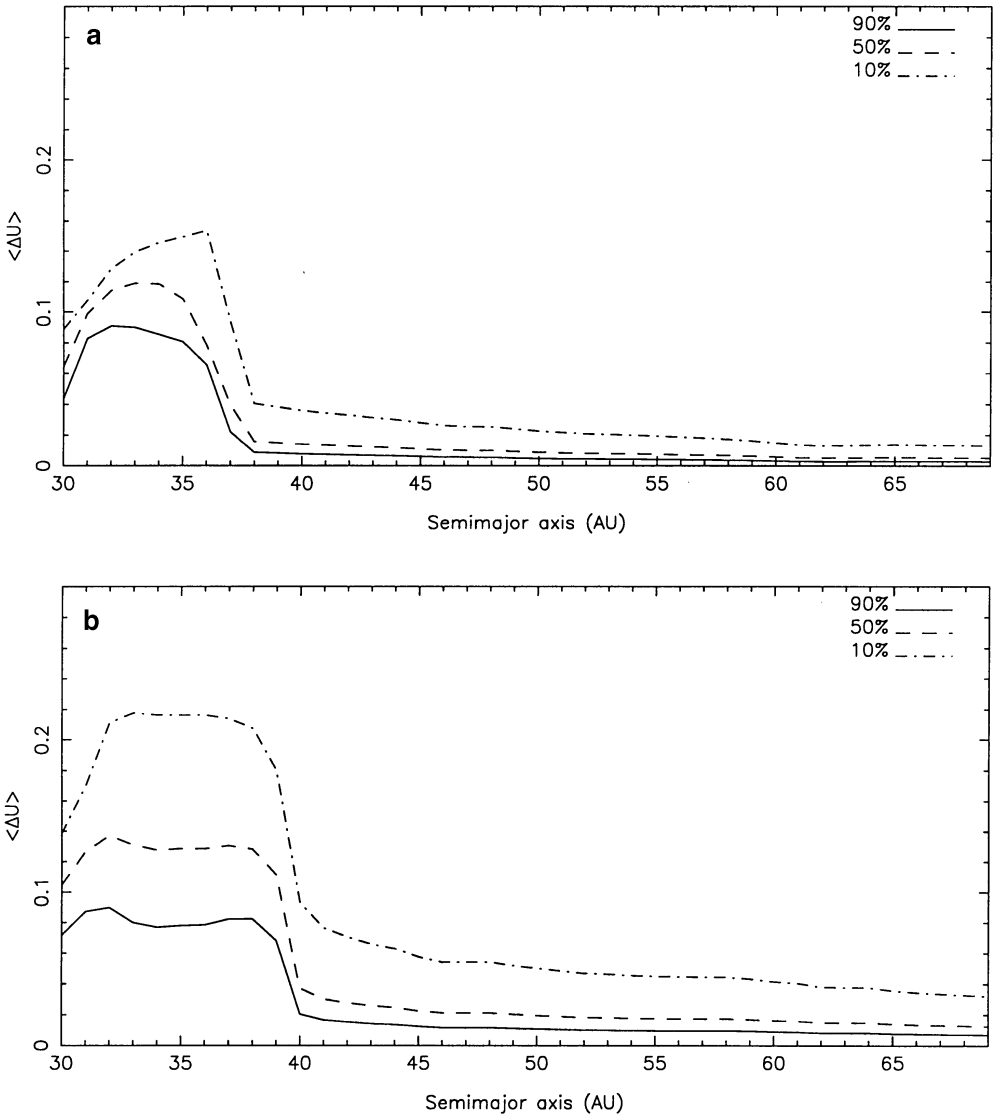

FIG. 2. Velocity excitation estimate of the Edgeworth–Kuiper belt from closest encounter with 3 planetesimals of mass 1.5 $M_{\oplus}$, on the average orbit of either set I (a) or set II (b).

why no object has been observed in the stable region between 36 and 39 AU (eccentricity less than 0.05). In fact we estimate that only a few percent of particles would keep an eccentricity smaller than 0.05. We recall, however, that these estimates of the excitation are very pessimistic (see end of Section II.B) and that we must resort to direct numerical simulations to give quantitative estimates.

Around 42–43 AU, the median excitation in velocity is slightly larger than 0.04, corresponding to an eccentricity of 0.06 and an inclination of 2°. To our knowledge our model is the only one proposed up to now that predicts an inclination excitation beyond 42 AU. The values produced by this model are of the same order of magnitude as the observed ones; the currently observed median eccentricity is 0.07. However, one must be aware that the observed distribution of eccentricity is probably biased toward large values since objects are more easily visible at perihelion, but on the other hand there exists a cutoff around 0.15 due to dynamical instabilities. It is not clear whether this would make the currently observed value an over- or an underestimate of the real primordial median eccentricity excitation. As for the inclination, the observed median value for EKBOs not in the 2 : 3 resonance is 4.0°. But a value of 6°–7° for the current unbiased median inclination can be expected using the bias estimate of Jewitt *et al.* 1996.

In the previous estimates, we have used the "average" orbital evolution of the integrated test planetesimals of set II, while the data show different categories of orbits. In our integrations of planetesimals, we recognize three types of orbits: most of the orbits (76% in set II) are injected into more tightly bound orbits and passed to Uranus, from where they probably evolve to orbits typical of Jupiter family comets (Levison and Duncan 1997). These planetesimals basically do not contribute to the

excitation of the EKB, not even the inner part, because their residence time is not long enough.

Another 9% of the planetesimals are scattered to large eccentric orbits with perihelion close to Neptune's orbit and survive for more than 100 Myr. We integrated these nine planetesimals for 1 Gyr, stopping the integration either when the perihelion distance became smaller than 20 AU (interaction with Uranus) or when the semimajor axis became larger than 10^4 AU, where the galactic tide would dominate the dynamics. Three planetesimals survived for 1 Gyr. To compare, in Duncan and Levison's simulation for the formation of the scattered disk (Duncan and Levison 1997) more than 30% of the planetesimals survive more than 100 Myr and 4% survive 1 Gyr. This validates our approach with the restricted three-body problem, and the difference between our numbers and theirs is probably due to the different initial conditions. All the particles of Duncan and Levison are initially on quite eccentric orbits with semimajor axis in the EKB, while ours are chosen on more circular orbits, favoring transfer toward Uranus and to the inner solar system. These "scattered" planetesimals are the ones responsible for the excitation of the classical EKB found in Fig. 2.

The last 15% of the planetesimals are stable over 100 Myr. They are not gravitationally scattered by Neptune, because of their trapping in some mean motion resonance with the planet, so they approximately keep their initial eccentricity and inclination. Due to their configuration, these planetesimals do not exceed 41 AU and therefore do not cross the classical EKB. In our simplified model, such planetesimals would survive for the age of the solar system. However, in a violent early solar system, with other large planetesimals crossing the region, they would probably be ejected from the protecting resonance on a much shorter time scale. The long residence time, together with the rather short orbital period of the planetesimal, implies a large number of crossings of the inner EKB (below 41 AU), hence creating a large excitation due to a small value of the minimum impact parameter b. This explains the shape of the curves in Fig. 2 for semimajor axis less than 41 AU.

In the second stage of our study, we want to give more quantitative estimates of the excitation produced by the LNSPs. For this reason we have integrated planetesimals with initial conditions as in set II, attributing them a mass of 1 $M_\oplus$, in the framework of the full three-body problem, Sun–Neptune–massive planetesimal. Neptune is initially taken to have its present orbit and present mass, as before. Integrations are followed for 100 Myr or until there is a collision between Neptune and the planetesimal, whichever occurs first. The orbital evolution of the planetesimals is found to be statistically similar to the previous case, with an increase of the number of planetesimals scattered on large eccentric orbits (16% instead of 9%). This yields a similar estimated excitation of the EKB due to the closest encounters. Using selected planetesimal evolutions as input for our modified SWIFT code, we integrated the evolution of sets of 500 test particles, initially on planar circular orbits with semimajor axis regularly spread between 35 and 55 AU.

In Fig. 3, we show the effect of a planetesimal of mass $M_p = 1\ M_\oplus$ on one of these "typical" short-lived orbits. In this

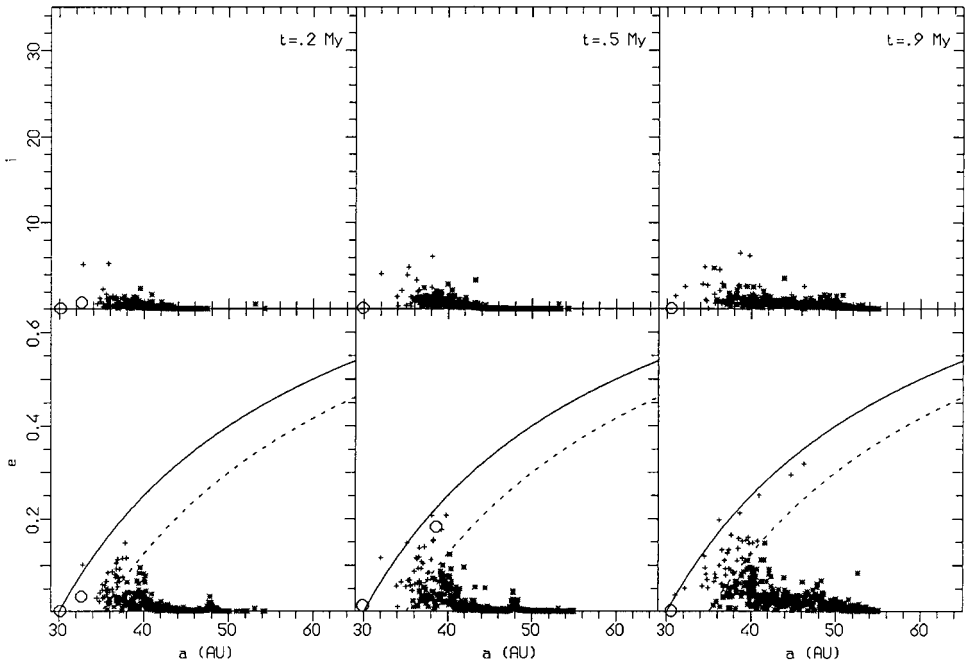

FIG. 3. Inclination (top row) and eccentricity (bottom row) versus semimajor axis of test particles at three different times (0.2 Myr, left; 0.5 Myr, middle; 0.9 Myr, right) for 500 test particles, due to the gravitational scattering of a planetesimal of mass 1 $M_\oplus$ on a short lived orbit. Crosses correspond to test particles entering the *scattered disk*, i.e., particles with perihelion distance less than 35 AU. The two circles represent Neptune (close to 30 AU, low inclination and eccentricity) and the planetesimal, no longer in the range of the plot in the third column ($T = 0.9$ Myr). Solid line: $q = 30$ AU; Dashed line: $q = 35$ AU.

particular case, the integration was stopped after 990,000 yr due to possible close encounter with Uranus, as described in Section II. The planetesimal spends some time in the inner part of the belt, exciting it to values that put half of the test particles in the scattered disk. It makes very few incursions into the classical belt, hence has almost no effect there. Assuming that most particles in the scattered disk will be ejected over the age of the solar system, we counted the number of particles with $q > 35$ AU and evaluated their median eccentricity and inclination. In the range [35, 40] AU (inner region), 46% of the particles survived, with $e_{\rm med} = 0.05$ and $i_{\rm med} = 1^\circ$. In the classical belt, it is convenient to distinguish between an intermediate region, [40, 47.7] AU, inside the 1 : 2 mean motion resonance with Neptune, and an outer region, beyond 47.7 AU. In the intermediate region all the particles survived, with $e_{\rm med} = 0.03$ and $i_{\rm med} = 0.6^\circ$. In the outer region, again all particles survived, with $e_{\rm med} = 0.03$ and $i_{\rm med} = 0.7^\circ$.

We next study the effect of a planetesimal of mass $M_{\rm p} = 1\ M_\oplus$ on a long-lived eccentric orbit. Figure 4 shows the eccentricity and inclination after 20, 50, and 100 Myr. The planetesimal evolves in the scattered disk and has an aphelion distance larger than 85 AU after 20 Myr and reaching 91.4 AU at the end of the integration. Since it penetrates very deep in the belt, it excites it to high eccentricity and inclination and actually ejects most of the test particles. No particle remains between 35 and 40 AU. In the region [40, 47.7] AU, only 4.3% of the initial population remain with $q > 35$ AU, with $e_{\rm med} = 0.19$ and $i_{\rm med} = 8.6^\circ$. Only in the outer region do we still have more than half of the original population (52%), but quite excited too: $e_{\rm med} = 0.27$ and $i_{\rm med} = 7.4^\circ$. In this region, the final mass depletion could be somewhat larger than the factor of 2 we see in the simulation, because particles close to the $q = 35$ AU boundary are unstable over 1 Gyr (Duncan *et al.* 1995) and the large eccentricities and inclinations result in intense collisional activity. The inclination, expressed in radians, is about half the eccentricity in the outer region, as expected from equipartition of energy. In this simulation, many particles ended in the scattered disk, with semimajor axis up to 350 AU. We also found four particles with orbits similar to that of 1996 TL66 ($a = 85$, $e = 0.59$, and $i = 24^\circ$) with a between 70 and 74 AU and eccentricity between 0.4 and 0.5, hence a perihelion distance just larger than 35 AU. We even found a particle with a very large semimajor axis, which never transited through the scattered disk: $a \sim 88$ AU and $e \sim 0.25$. This orbit was reached through a very close encounter with the planetesimal.

The excitation and mass depletion provided by a 1 $M_\oplus$ planetesimal may seem rather extreme. We then studied the case of a planetesimal of (1/10) $M_\oplus$ on the same long-lived excited orbit. In the modified SWIFT code, we used the same orbit for both Neptune and the planetesimal as in the previous case, but set the mass of the planetesimal to 1/10 $M_\oplus$. This was not self-consistent, since the orbit of Neptune is due to interactions with a more massive planetesimal, but it allowed us to get the desired kind of orbit at no extra cost. It also allowed us to see clearly the effect of the perturbing mass, with no change in the orbit. The results are shown in Fig. 5. The excitation is much smaller than in the previous case. In the present case, the inner region $a \in [35, 40]$ retains only 2.4% of the particles, with $e_{\rm med} = 0.01$ and $i_{\rm med} = 1.3^\circ$. The intermediate region

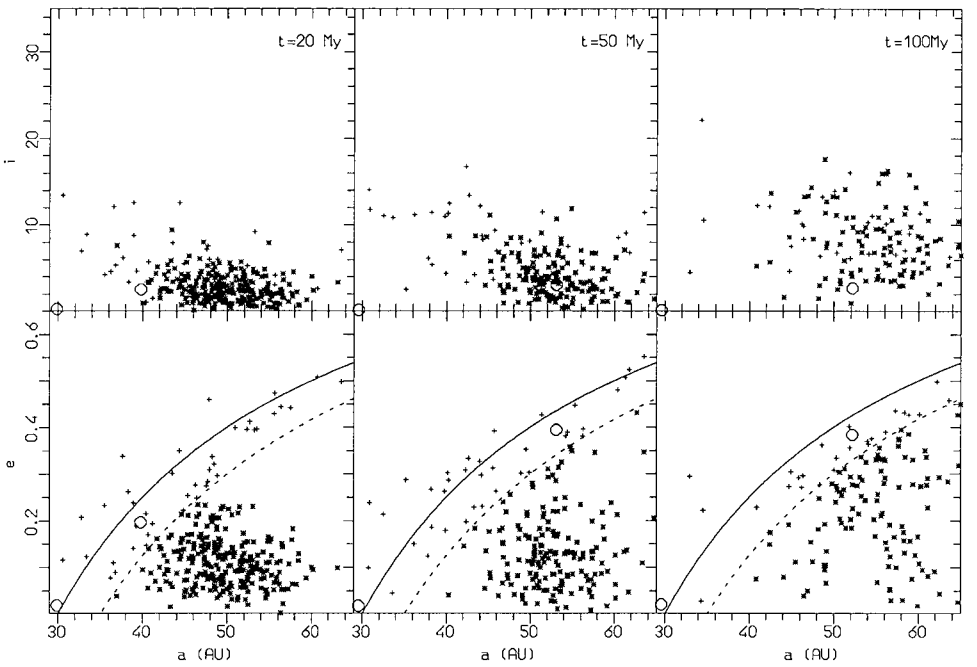

FIG. 4. Same as Fig. 3 but for a planetesimal on a scattered long-lived orbit lasting 100 Myr. Such a planetesimal has its perihelion close to 30 AU, while its aphelion reaches, during the evolution, 90 AU.

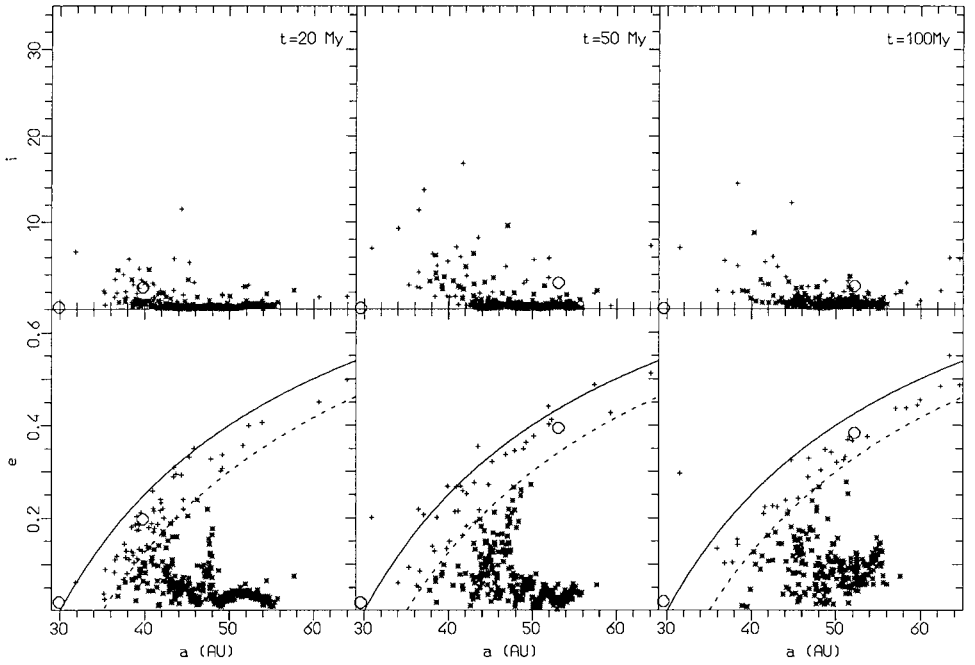

FIG. 5. Same as Fig. 4 but for a planetesimal of mass $1/10\ M_{\oplus}$.

is much more populated with 29% of the particles, $e_{\rm med} = 0.16$, and $i_{\rm med} = 0.8^{\circ}$. Almost all the particles (98%) remain in the outer region, with $e_{\rm med} = 0.06$ and $i_{\rm med} = 0.6^{\circ}$. Note in particular the almost negligible excitation in inclination. For particles with $a > 40$ AU, the inclination is about 10 times smaller than the eccentricity, far from equipartion of energy.

Finally, we simulated the effect of a planetesimal of mass $1\ M_{\oplus}$ on one of the long-lived stable orbits. Such a planetesimal spends all its time in the inner part of the belt, hence having very little effect on the outer part. On Fig. 6 we clearly see the excitation of particles interior to about 43 AU, with many of them going into the scattered disk. For particles out of 45 AU,

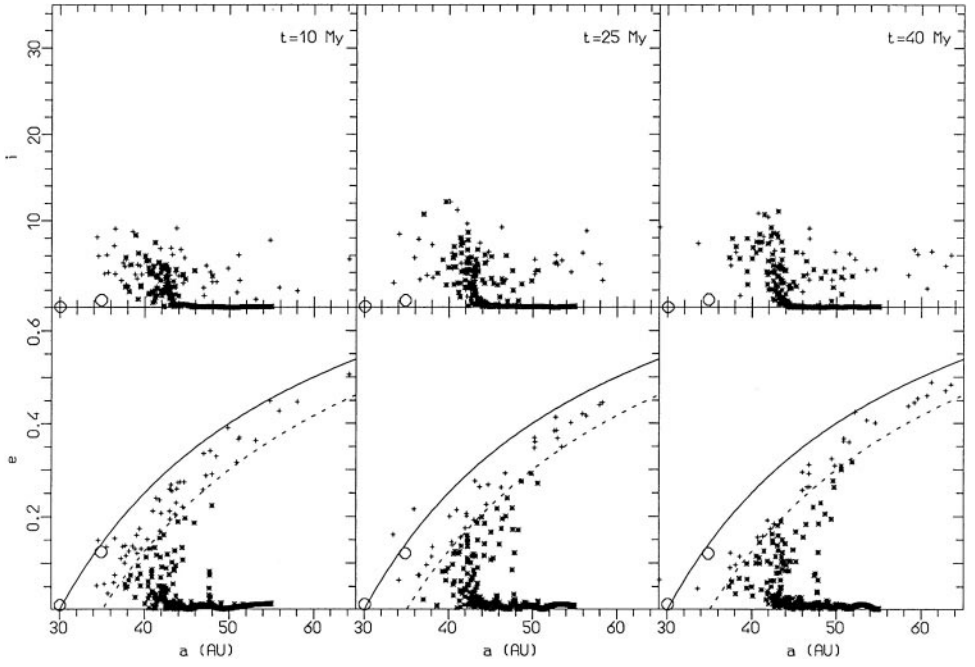

FIG. 6. Same as Fig. 3 but for a planetesimal on a stable long-lived orbit. The planetesimal is locked in a mean motion resonance with Neptune and keeps a semimajor axis of about 35 AU.

we see the secular oscillation of eccentricity and an increase of eccentricity in the 2 : 1 mean motion resonance with Neptune. The strong eccentricity excitation in the resonance was only slightly visible at the beginning of the simulations in Figs. 4 and 5 but then was hidden by the globally strong excitation. Moreover, the effect of the resonance is even more reduced by the large fluctuations of the position of Neptune. In the present quiet case, all particles outside 47.7 AU are kept, with $e_{\rm med} = 0.03$ and $i_{\rm med} = 0.04^\circ$. In the intermediate region, only 1% is lost, and $e_{\rm med} = 0.02$ and $i_{\rm med} = 0.02^\circ$. Only in the inner region do we have a very large mass depletion, with only 5.6% of the particles retained, with $e_{\rm med} = 0.05$ and $i_{\rm med} = 5.6^\circ$. The mass depletion of the inner region is much larger here than in Fig. 3 because the gravitational interaction with the planetesimal lasts 100 Myr, about 200 times longer than in the previous case.

The primordial existence of large planetesimals is predicted by modern models of planetary formation. Fernández and Ip (1996) show that the accretion of Neptune requires the presence of a mass as large as 60 $M_\oplus$ in Neptune's environment, and predict also the formation of planetesimals with masses in the range 1 to 5 $M_\oplus$. Moreover, the obliquity of the spin axis of Uranus implies that a collision with a primordial planetesimal of about 1 $M_\oplus$ must have occured in the final stages of planetary formation (Safronov 1966, Parisi and Brunini 1996) and thus indicates that planetesimals of a few Earth masses should not have been rare in the primordial outer Solar System.

A point of concern is that the existence of large planetesimals could have excited the eccentricity of Neptune beyond the observed value. Figure 7 shows statistics of the final eccentricity (left panels) and inclination (right panels) of Neptune due to the planetesimals injected towards Uranus (top), the nonscattered planetesimals (middle), and the planetesimals scattered to large eccentric orbits (bottom). We remark that the highest inclination reached is just 0.5°, which is of the order of the present inclination. Concerning the eccentricity, starting with the present 0.008 value, we get at most 0.047. This eccentricity is higher than the maximum eccentricity reached by Neptune during its secular oscillation (0.02), but could have easily been damped by encounters with small bodies (Lissauer and Stewart 1993).

IV. JUPITER-SCATTERED PLANETESIMALS

We now apply the same method to investigate the excitation that large Jupiter-scattered planetesimals could have provided to the primordial asteroid belt.

Figure 8 shows the minimal excitation (ΔU), estimated from the closest encounter, due to five planetesimals of mass 1 $M_\oplus$ assumed to follow the "average" evolution of the integrated test planetesimals of set III. We remark that there is a nonnegligible excitation in the outer belt, beyond 3 AU, but very little excitation in the main belt between 2 and 3 AU. Increasing the number N and mass $M_{\rm p}$ of planetesimals would scale the curves in Fig. 8 roughly as $M_{\rm p}\sqrt{N}$. However, any choice of N and $M_{\rm p}$ would result in a gradient of the excitation with respect to semimajor axis in the 2 to 3.5 AU range, a feature not observed in the present asteroid belt. This is due to the very short median dynamical lifetime for 10^4 yr for the scattered planetesimals, resulting in very few having the possibility of decreasing their perihelion distance and crossing the inner belt. This is a major difference from the case of the LNSPs, because Neptune, being 20 times smaller than Jupiter, is able to scatter some planetesimals to large eccentric orbits and keep them on these orbits for a long time, up to 1 Gyr in some cases.

The larger excitation between 3.5 and 4.5 AU is due to the 15% of the integrated planetesimals that are not scattered by Jupiter during the 1 Myr of integration. Therefore, the number of passages of these bodies in the 3 to 5 AU region is very large. This is similar to what occurs with the LNSPs and produces the large excitation in the 30 to 40 AU region. If one of these still unscattered planetesimals ever gets scattered by Jupiter, it will presumably follow a very rapid evolution toward ejection, therefore not contributing significantly to the excitation of the main asteroid belt.

Here again, we verify our understanding of the excitation process with a direct simulation. We choose a planetesimal representative of what happens in set III. Its mass is 1 $M_\oplus$, and it enters the asteroid belt for a little less than 300,000 Yr, then goes on an orbit with pericenter larger than 6 AU, and finally escapes on a hyperbolic trajectory. We integrated the time evolution of 100 test particles, initially on circular orbits with semimajor axis uniformly distributed between 2 and 3.5 AU, and inclination evenly distributed between 0 and 1°. Figure 9 shows three snapshots at 0.05, 0.15, and 0.3 My, similar to those of Fig. 3. On the bottom row, we have plotted the line of aphelion distance of 4.1 AU (solid line) above which an asteroid would be unstable on a very short timescale due to interactions with Jupiter, except in mean motion resonances. The dashed line represents a perihelion distance of 1.7 AU, below which an asteroid would strongly interact with Mars. We plotted snapshots only up to 0.3 My since the planetesimal does not enter the asteroid belt after that time. The general result is similar to what we found in Fig. 8, but with a faster and larger excitation. For particles outside 3 AU, the excitation is very large, exceeding 0.4 in eccentricity, but there is very little excitation in the inner part, and we can see a definite gradient of eccentricity excitation between 2 and 3 AU. A very important point is the very low inclination excitation, barely reaching 3° when an equipartition of energy would imply an inclination of order 10° in the outer region. In this scenario, the mass depletion is rather small: only 4% of the test particles were ejected before the planetesimal left the asteroid region, and three test particles became Mars crossers. The ejected test particles all had an initial semimajor axis larger than 3 AU. In addition, we note a large variation in semimajor axis of the test particles. At the end of the integration, only 17 test particles were outside 3 AU, while there were 34 originally. Adding this to the ejected particles, this means that 14 particles had a large enough change in semimajor axis to push them below 3 AU. The median change in semimajor axis Δa of the

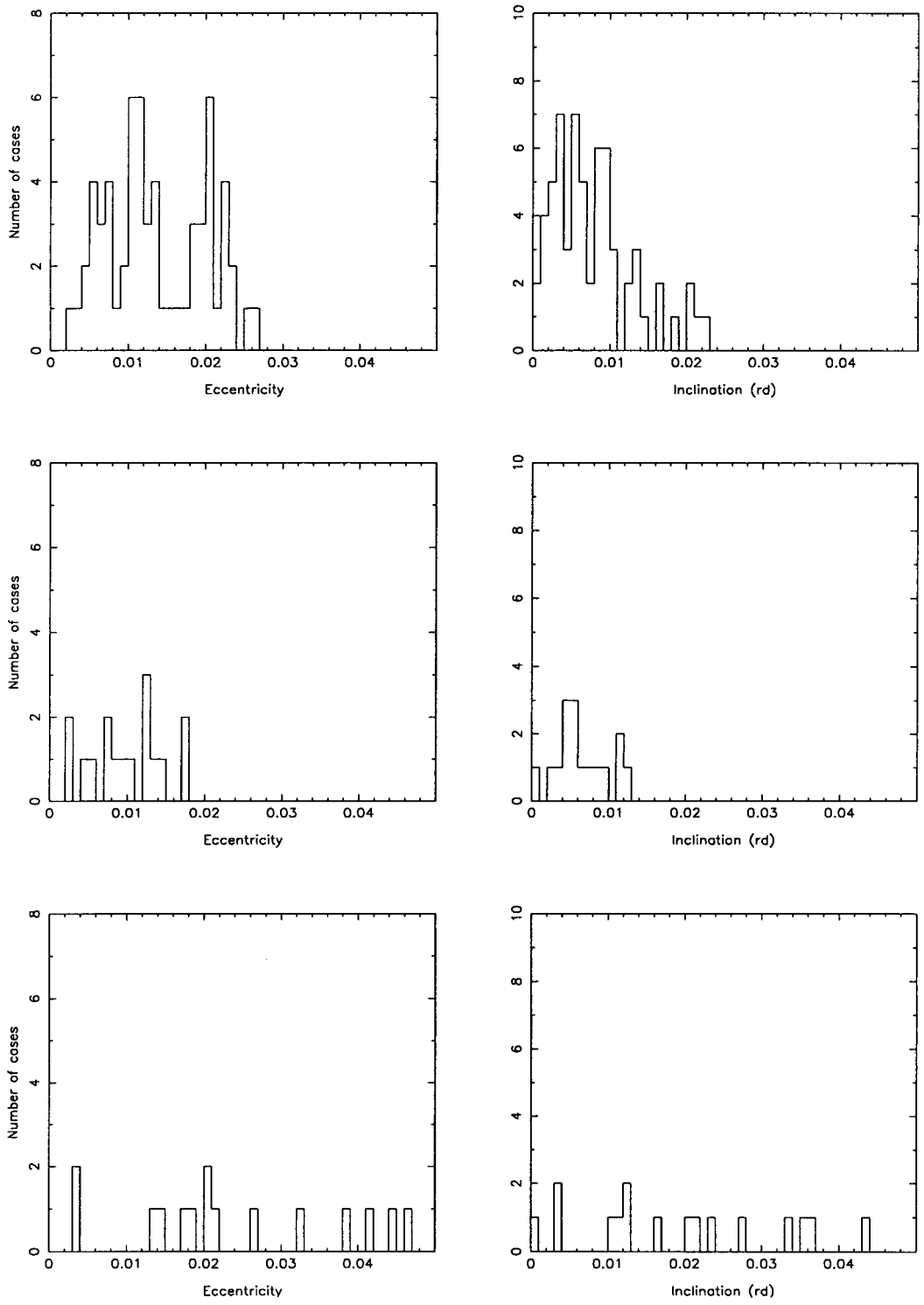

FIG. 7. Distribution of the final eccentricity (left panels) and inclination (right panels) of Neptune due to the planetesimals injected toward Uranus (top), the nonscattered planetesimals (middle), and the planetesimals scattered to large eccentric orbits (bottom). The planetesimals have a mass of $1 M_{\oplus}$, and the motion was integrated for 100 Myr.

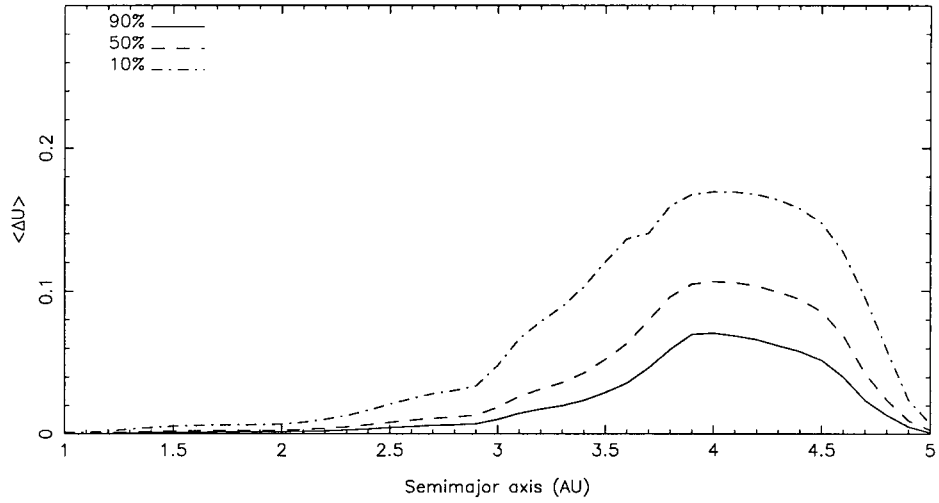

FIG. 8. Velocity excitation estimate of the asteroid belt from closest encounters with five planetesimals of mass 1 $M_\oplus$, on the average orbit of set III.

remaining particles is 0.05 AU, while 6% of the particles moved by 0.5–0.6 AU.

This result on the global inefficiency of the LJSPs in structuring the belt as it is now confirms the previous conclusions reached by Ip (1987) with a Monte Carlo model. To overcome the problem of the very short dynamical lifetime of the scattered LJSPs, Ip proposed that the excitation of the primordial belt was provided by the LJSPs scattered during the late growing phase of Jupiter's core. Jupiter being smaller, its efficiency in ejecting bodies would be reduced by a large amount. For this reason, we have integrated the evolution of LJSPs for 10 Myr, during which time we increase Jupiter's mass linearly from 5 to 15 $M_\oplus$. Of the planetesimals, 98% survived for that time. We stopped the integration after 10 Myr, because the accretion of gas becomes very fast once Jupiter's core has reached 15 $M_\oplus$ (Pollack *et al.* 1996), with Jupiter reaching its present mass in only a few 10^5 yr. From that moment on, the following evolution of LJSPs would be analogous to that simulated above. The excitation provided to the asteroids by five planetesimals of 1 $M_\oplus$ during the accretion phase of Jupiter's core is illustrated in Fig. 10. Beyond

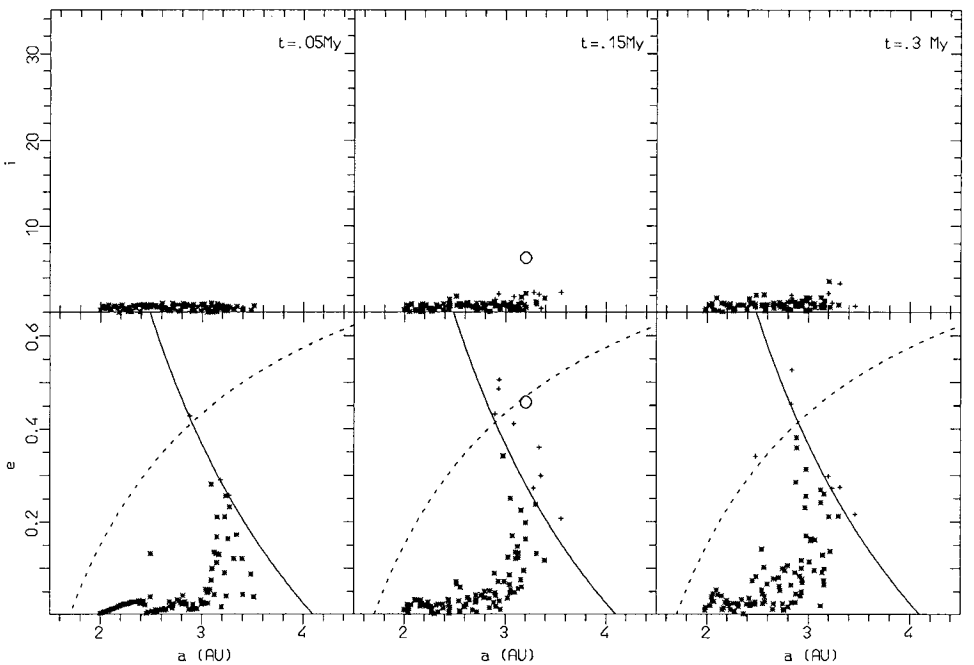

FIG. 9. Same as Fig. 3 but for a planetesimal scattered by Jupiter, on an orbit typical of set III. Crosses denotes particles with either $q < 1.7$ AU or $Q > 4.1$ AU. Solid line: $Q = 4.1$ AU; dashed line: $q = 1.7$ AU.

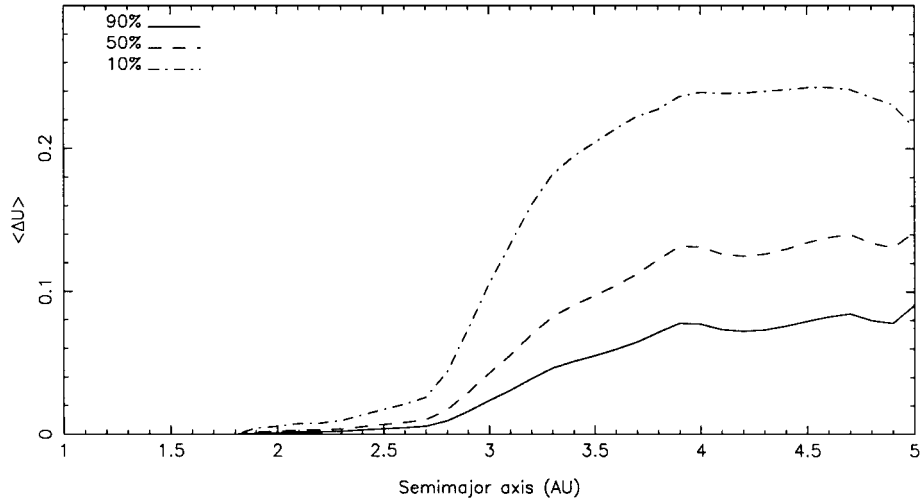

FIG. 10. Same as Fig. 8 but for set IV.

3 AU, the excitation is larger than in Fig. 8, due to the increased residence time of the planetesimals. Conversely, no planetesimal decreased its perihelion distance below 1.8 AU because the small Jupiter's core is less efficient in scattering the planetesimals. The excitation between 1.8 and 2.7 AU is still very limited and shows a gradient with increasing semimajor axis, similar to that in Fig. 8. Therefore, we can conclude that LJSPs can explain the mass depletion and excitation of the outer belt ($a > 3.28$ AU), but certainly not the excitation of the inner and central parts of the belt. This is in contrast with the results obtained by Ip (1987). We believe that his success was an artifact of the Monte Carlo model he used, which probably overestimated the residence time of LJSPs in the inner and central parts of the belt.

In order to obtain scattered planetesimals on long-lived orbits in the main belt, Wetherill 1989 proposed another mechanism. Due to mutual gravitational interactions, some LJSPs could decrease their eccentricity, isolating themselves in the main asteroid belt safe from close encounters with Jupiter (see Introduction). We have performed 100 integrations of a system composed of the present Jupiter and five planetesimals of 1 $M_\oplus$, choosing their initial conditions at random among those of set III for each integration. Each system is integrated for 1 Myr, taking into account all mutual gravitational interactions, with a Bulirsh and Stoer N-body integration code.

At the end of 14% of the integrations, one of the planetesimals is found to be decoupled from Jupiter. This means that its aphelion distance had dropped below 4.4 AU (where encounters with Jupiter become rare). Among those, eight planetesimals have penetrated the main belt, with a perihelion distance below about 3.28 AU; we continued the integrations of these cases for another 1 Myr. One of the planetesimals did not survive. Of the remaining seven cases, only six had a planetesimal crossing the entire asteroid belt. However, three of them reached 1 AU and therefore would have prevented the accretion of terrestrial planets, and we have thus disgarded them. One of the remaining is deeply anchored in the belt, with semimajor axis of about 2.8 AU, just outside the 5 : 2 resonance with Jupiter, and an average eccentricity of 0.28. Even in a realistic model of the Solar System, this 1 $M_\oplus$ planetesimal would not leave the asteroid belt and would still be observed. This case is also not considered as a possible history for our Solar System. We are left with only two integrations out of the 100 performed having a planetesimal decoupled from Jupiter that (i) crosses the entire asteroid belt, (ii) does not affect the region of the inner planets, and (iii) is in a region dynamically unstable on a moderately long time scale (one in the 2 : 1 resonance, the other in a rather chaotic region at large eccentricity) leaving the planetesimal time to excite the asteroids, but eventually allowing it to escape.

Figure 11a presents the minimum excitation of the asteroid belt received from the closest encounter with one of these planetesimals during the 2-Myr integration. Figure 11b estimates the excitation assuming that this planetesimal remains on its final orbit for 400 Myr before leaving. For a shorter residence time, the result would be intermediate between Fig. 11a and Fig. 11b. The excitation scales roughly as the square root of the number of passages, and hence of the residence time. Comparing this with the observed structure of the asteroid belt presents a puzzle and requires a quantitative estimate of the excitation.

As explained above, this can be obtained only by direct numerical simulation of the gravitational interaction of both the giant protoplanet and the planetesimal with the test particles. In the present case we used the standard SWIFT code, taking Jupiter on its present orbit and the planetesimal on the orbit reached after 2 My in the integration used for Fig. 11a, namely $a \sim 3.1$ AU, $e \sim 0.33$, and $i \sim 3.5^\circ$. We did not need to use the modified SWIFT code since the orbit of the planetesimal does not encounter Jupiter, and it was very easy to just integrate the equations of motion directly. (Actually this simulation was used to test the modified SWIFT code, as explained in Section II.C).

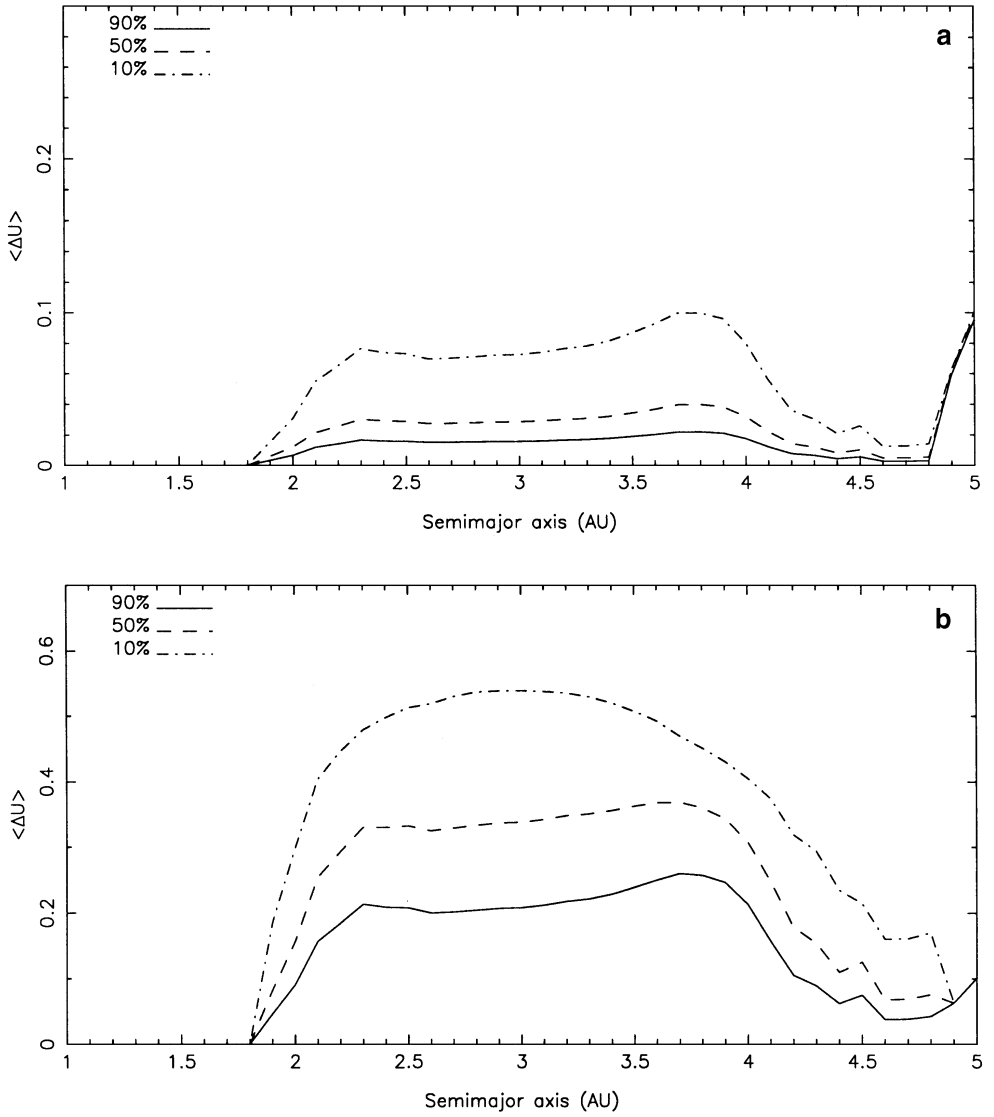

FIG. 11. Velocity excitation estimate of the asteroid belt from closest encounters with 1 planetesimal of 1 $M_\oplus$, on one of the orbits decoupled from Jupiter, obtained in 2% of the integrations. The residence time is either 2 Myr (a) or 400 Myr (b).

The initial conditions of the test particle are the same as those used for the simulation of Fig. 9. After only 1 My, the excitation is already very large, somewhat similar to the currently observed excitation of the asteroid belt, both in eccentricity and in inclination. In this case, the inclination excitation is of the same order of magnitude as the eccentricity excitation, corresponding to an equipartition of energy, contrary to what we noted in Fig. 9. This excitation is also close to that of Fig. 11b after 400 My. The particles fill the region below the solid and dashed lines, with a few particles already going into the Mars- and Jupiter-crossing regions. At 3 and 5 My, more particles are found in the Mars- and Jupiter-crossing regions and many have already escaped from the solar system. The few particles remaining in the stable region below the dashed and solid lines are still well spread over the entire region. The mass depletion is 71% after 5 My for all the particles in the simulation and reaches 84% if we count only particles in the stable region. Only four particles remain with semimajor axis larger than 3 AU. It is interesting to note that continuing the integration leads to ejection of all test particles after about 50 Myr.

The direct simulation shows that the planetesimal efficiency in depleting and exciting the asteroid belt is 100 to 400 times larger than estimated by taking into account only the closest encounters. This is because in the direct simulations we correctly account for the dynamics driven by Jupiter: regular oscillations in eccentricity outside of mean-motion resonances and stronger oscillations both in eccentricity and inclination inside mean-motion resonances. The planetesimal interacts with this in two ways. First, through close encounters it allows the test particles to suddenly jump in semimajor axis, hence going from one

oscillation in eccentricity to another one, with possibly a larger proper eccentricity. In particular, particles can enter the strong mean motion resonances, increase their eccentricity, and then be extracted from the resonances. The second effect is the dynamics driven by the planetesimal itself. Its mass is smaller than Jupiter's mass, but it is closer to the particles, and its eccentricity and inclination are much larger, hence producing a strong perturbation. Trying to understand the combined effect of Jupiter and the planetesimal from the effect of each one alone is not trivial; at present we rely on the direct numerical integrations. The changes in semimajor axis resulting from the very complex influence of the planetesimal also might explain the observed radial mixing of different taxonomic types. In the present simulation, the median change Δa (between initial and final values) is 0.26 AU for the remaining particles, with 11% of the particles having Δa between 0.5 and 0.8 AU. The difference between the maximal and the minimal semimajor axis ever reached during the evolution is often larger than 1 AU.

As in the case of Neptune, we also simulated the effect of a smaller planetesimal ($1/10\ M_\oplus$) on a similar orbit. We use the same initial conditions as for Fig. 12 and integrate the full equations of motion. The result is plotted on Fig. 13. After 16 My, the distribution is similar to the distribution of Fig. 12 at 1 My. Here again, the only important evolution between the three snapshots is the drift of particles to large eccentricities in the planet-crossing regions. After 48 My, the mass depletion is only 49% for all the particles and 61% for those in the stable region. Beyond 3 AU, only 9 particles out of the initial 34 survived. From Eq. (2), we see that the closest encounters give an effect roughly proportional to the mass of the planetesimal, at least for the small velocity excitations. Here, the decrease in efficiency is by more than the factor of 10 between the masses of the planetesimals. This again results from the complex interplay between the "random walk" due to the gravitational scattering by the planetesimal, and the dynamics driven by Jupiter. At the same time, the excitation in semimajor axis is only divided by 2 for the remaining particles: median $\Delta a = 0.13$, and 8% of the particles between 0.3 and 0.5 AU. But these values are measured after about 50 Myr, a factor of 10 longer than in the previous case, and there are still twice as many particles. We also note that although starting on a stable orbit, the planetesimal increases its eccentricity up to the Mars crossing region, while its inclination decreases. Since its mass is equal to that of Mars, it is difficult to know what would occur next. But it seems clear that on a few tens of million years time scale, such a planetesimal becomes unstable and leave the asteroid belt.

Using the direct numerical integrations, we also tested the crucial part of the Monte Carlo approach: the statistics of close encounters. Using the simulation with the martian-sized planetesimal, we counted the number of close encounters with impact parameter less than a given b over 2 My. In this case, the eccentricity and inclination of the particles are not yet excited, and we reproduce the conditions assumed in the Monte Carlo approach. Our estimate of the number of encounters as a function of b, as explained in Section II.B, perfectly matches the numbers measured in the direct simulations, thus proving that the encounter statistics used in our Monte Carlo code is correct. The difference between the results obtained with the Monte Carlo and with the direct integration therefore must be due to the effect of

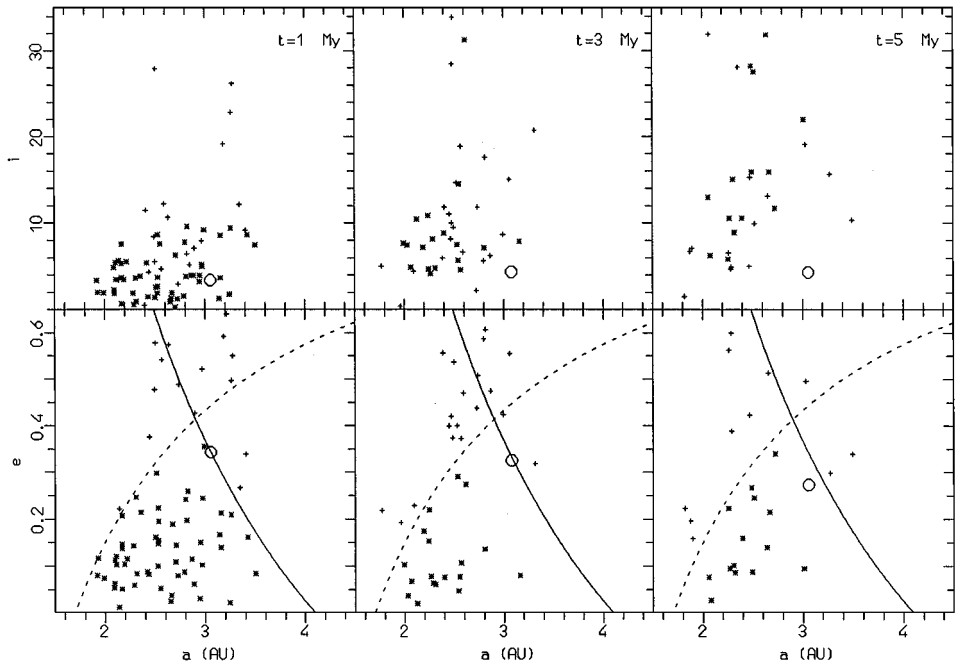

FIG. 12. Same as Fig. 9 but for the decoupled planetesimal of Fig. 11a.

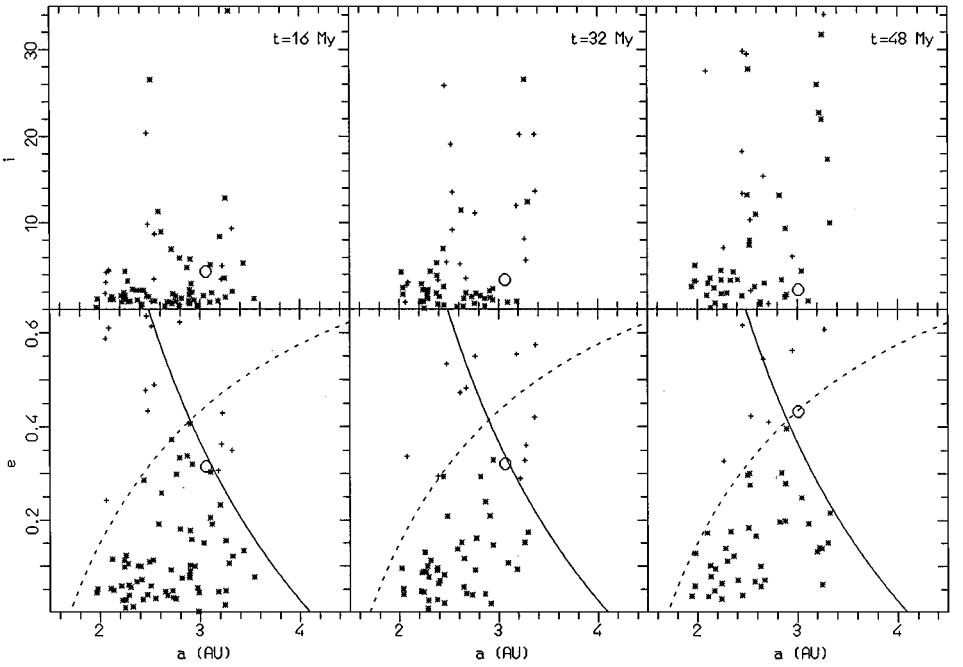

FIG. 13. Same as Fig. 12 but for a planetesimal of mass $1/10\ M_\oplus$. Same initial conditions as in Fig. 12.

cumulative encounters and to the interplay with the resonant and secular dynamics induced by Jupiter and by the planetesimal.

V. DISCUSSION

The primordial existence of large planetesimals is predicted by modern models of planetary formation. This seems confirmed by the large obliquity of the spin axes of the giant planets (in particular Saturn and Uranus), for which the generally accepted explanation is collision with a primordial planetesimal of about $1\ M_\oplus$ occuring in the final stages of planetary formation. In this paper, we have investigated the role that large planetesimals scattered by giant planets could have had in exciting the asteroid and Edgeworth–Kuiper belts. This has been done using both Monte Carlo simulations and direct integrations. Comparison between the results obtained with the two methods has shown limitations on the applicability of Monte Carlo methods. In terms of both mass depletion and excitation of remaining bodies, the Monte Carlo approach gives results that are two orders of magnitude too low. The Monte Carlo method cannot reproduce the complex interplay between the perturbations of the planetesimal, and the intrinsic dynamics due to the giant protoplanet (see Sect. IV, and the discussion on Pallas below). The Monte Carlo approach can only tell us for which parameters we can obtain measurable effects, but we then need to resort to direct integrations to get quantitative answers.

We have shown that depending on the mass and dynamical evolution of the planetesimal, we can get a large variety of final orbital distributions for the small bodies. Hence, this work cannot be directly predictive in the sense of telling us what we should see. It will however help us to recontruct what really happened in the early ages of the solar system from the present observed structure of the small body belts. Unfortunately, knowledge of the structure of the Edgeworth–Kuiper belt is still very sparse, so the restrictions on the primordial evolution are loose. On the contrary, the wealth of data already obtained on the asteroid belt should allow us to derive stronger constraints.

For the EKB two features seem to be established: a large mass depletion in the region 30–50 AU and a considerable orbital excitation in the same region (see the Introduction). No existing models could explain the observed orbital excitation in the 40–50 AU range, while the only proposed mechanism for mass depletion relies on collisional erosion. We show that planetesimals scattered by Neptune on elliptic orbits could easily have provided both the dynamical excitation and the mass depletion of the EKB. With a planetesimal of $1\ M_\oplus$ acting for 100 My the mass depletion and the excitation of the EKB up to 50 AU are very large (Fig. 4). It seems that even planetesimals of a fraction of $1\ M_\oplus$ could have produced the belt's structure (as characterized by present observations). Nevertheless, none of our simulations exactly reproduces the observed belt, for the following reasons.

First, the 2 : 3 mean motion resonance with Neptune (39.5 AU) is not associated with an evident concentration of surviving small bodies. The estimated population of the 2 : 3 resonance is 10–15% of the total population up to 50 AU (Jewitt *et al.* 1998). It is possible that some of the bodies in the 2 : 3 resonance constitute a "Pluto family," produced by the breakup of the Pluto–Charon parent body (Stern *et al.* 1999), in which case the primordial ratio between particles in the 2 : 3 resonance and particles in

the 40–50 AU region would be much smaller than 10%. In the case of Fig. 4, assuming a 10% ratio, we should expect about two particles in resonance. So the lack of particles in the 2 : 3 resonance could just be a problem of small-number statistics. Nevertheless, it is true that the process we study here rarely injects particles into the resonances of the inner belt and keeps them there. As soon as the particles are excited by the planetesimal, they are quickly removed by encounters with Neptune, with the exception of those in mean motion resonance. But the latter are easily removed from the resonances by subsequent close encounters with the planetesimal. Also, Neptune's semimajor axis changes rapidly due to encounters with the planetesimal, the change sometimes exceeding 0.1 AU over a 20,000-y typical libration period in the 2 : 3 resonance. Over the 100 My integration time, Neptune's semimajor axis changes several times by up to 0.6 AU due to successive encounters with the planetesimal. This changes the location of the stable part of the resonance in both semimajor axis and phase. All this makes it relatively improbable that particles trapped in the resonances survive until the final ejection of the massive planetesimal. Adding an adiabatic migration of Neptune at the same time would not help here: as long as the massive planetesimal is in the system, multiple encounters and jumps of Neptune's semimajor axis would still prevent any permanent adiabatic capture into resonance. Hahn and Malhotra (1999) showed that even the migration of Neptune under the effect of lunar mass planetesimals is not adiabatic enough to allow permanent capture into resonance. The precise limits of the process of adiabatic capture into resonance are presently under investigation. However, we can imagine a two-stage process: a large planetesimal scattered by Neptune first excites and depletes the belt and a subsequent adiabatic migration of Neptune, occuring after the ejection of the large planetesimal, finally captures a fraction of the bodies into resonance, as in Malhotra's scenario (1995). In this case, we cannot deduce the migration range of Neptune from the eccentricity distribution of the bodies in the resonance because this process would capture an already excited population. A small migration of Neptune (1 or 2 AU) could be sufficient here since we do not have to excite the belt. Note that even this scenario is not straightforward, as Malhotra (1993) showed that the probability of capture into resonance is a steep decreasing function of the particle eccentricity.

Second, no body has yet been found in the classical belt with semimajor axis larger than about 50 AU. After an analysis of observational biases, this led Jewitt *et al.* 1998 to propose the possibility that the belt "ends" at about 50 AU, although Gladman *et al.* 1998 claim that the observations still do not require this conclusion. According to our excitation scenario, the absence of discovery beyond 50 AU would be a problem. Actually, even assuming a primordial belt of small extent (the initial population extended only to 55 AU in the simulations), the particles would be scattered to outer regions by close encounters with the planetesimal. In Fig. 4 we see particles up to 65 AU with eccentricities up to 0.5. We cannot imagine an easy way to solve this paradox. If future observations confirm the absence of bodies beyond 50 AU, this will become a crucial constraint.

Our results on the strong excitation provided by Mars- to Earth-sized planetesimals raise the natural question of the effect of Pluto on the stability of the plutinos (bodies in the 2 : 3 resonance). We have integrated, with and without Pluto, the 4 giant planets and 50 test particles in the 2 : 3 resonance ($a = 39.5$ AU) uniformly distributed between 0 and 0.3 in eccentricity, between 0° and 15° in inclination (uniform distribution of cosine), and between 0° and 360° in Ω and ϖ, and with $\sigma = 3\lambda - 2\lambda_{\text{Neptune}} - \varpi$ between 180° and 330° to have all possible libration amplitudes. There is a natural decay of the population (Morbidelli 1997) due to chaotic evolution. The decay curves are statistically equivalent in both simulations over 1 Gy. This shows that Pluto has no noticeable effect on the global population of the 2 : 3 resonance. It seems that it may significantly affect only particles on orbits with eccentricity and inclination very similar to its own (Nesvorny, private communication).

Concerning the asteroid belt, large Jupiter-scattered planetesimals are effective in depleting the outer belt ($a > 3.28$ AU) but not in exciting the inner and central belts (Fig. 9). Very few LJSPs cross the entire belt, and those which do so have very short dynamical lifetimes. We have then explored the possibility proposed by Wetherill (1989) that some planetesimals get decoupled from Jupiter by mutual gravitational interactions. These objects would cross the entire asteroid belt for a long time, providing a large global excitation. The simulations of Fig. 12 and Fig. 13 both lead at some time to a qualitatively correct population of asteroids. Of course we are not able to "reproduce" the real asteroid belt, but we produce its most important features. The results are reasonable in terms not only of eccentricity and inclination excitation, and mass depletion, but also in terms of radial mixing (median $\Delta a \in [0.13; 0.26]$). Another very interesting result is the possibility of obtaining bodies on Pallas-like orbits. In Fig. 12, we see three particles with inclination around 30°, semimajor axis between 2.4 and 2.7 AU and moderate eccentricity (0.14 to 0.27). In particular, one of them has osculating orbital elements at the end of the simulation: $a = 2.64$ AU, $e = 0.14$, and $i = 31.8^\circ$. The other two particles have a slightly lower osculating inclination around 28° and semimajor axis around 2.5 AU, but they are both out of the 3 : 1 mean motion resonance with Jupiter. To our knowledge, this is the first time that a model has generated Pallas-like objects. The typical path to reach this kind of orbit is as follows. Particles are injected into the 3 : 1 resonance by perturbations from the planetesimal. Subsequently, they chaotically evolve under the influence of the resonance, with large variations in eccentricity and inclination. Finally they are extracted from the resonance by a close encounter with the planetesimal in a high i, low e state. This happens not only in the case of the Earth-mass planetesimal, but also in the case of the Mars-mass planetesimal, although in the latter case the final semimajor axis of these Pallas-like objects is closer to the transporting resonance. We observe other particles following similar paths, but extracted on moderate inclination orbits. During their

stay in the resonance, they can temporary reach eccentricities larger than 0.9. Finally they are extracted with moderate eccentricities less than 0.4. Hence these bodies are likely to have been heated by solar radiation at their perihelion (<0.3 AU) at some time in their history, even though they are finally located in a rather cool region.

All these results are very encouraging, except for the small probability that a planetesimal is decoupled from Jupiter, which occurs in only 2% of the simulated cases. Moreover, the resulting belt depends critically on the mass and dynamical lifetime of the decoupled planetesimal. It is somewhat uncomfortable to conclude that the present structure of the asteroid belt depends on a rather improbable mechanism, so we believe that other scenarios should be looked for. The one proposed by Wetherill (1992) (see Introduction) seems to be promising, and we plan to investigate this possibility in a forthcoming paper.

ACKNOWLEDGMENT

Part of this work was performed using the computing facilities provided by the program "Simulations Interactives et Visualisation en Astronomie et Mécanique (SIVAM)."

REFERENCES

Arnold, J. R. 1965. The origin of meteorites as small bodies. III. General considerations *Astrophys. J.* **141**, 1548–1556.

Barucci, M. A., D. J. Tholen, A. Doressoundiram, M. Fulchignoni, and M. Lazzarin 1998. Spectroscopic observations of Edgeworth–Kuiper Belt (EKB) objects. *Bull. Am. Astron Soc.* **30**, 1112.

Chambers, J. E., and G. W. Wetherill 1998. Making the terrestrial planets: *N*-body integrations of planetary embryos in three dimensions. *Icarus* **136**, 304–327.

Davis, D. R., and P. Farinella 1998. Collisional erosion of a massive Edgeworth–Kuiper belt: Constraints on the initial population. *Proc. Lunar Planet. Sci. Conf. 29th*, 1437.

Davis, D. R., C. R. Chapman, R. Greenberg, S. J. Weidenschilling, and A. W. Harris 1979. Collisional evolution of asteroids, populations, rotations and velocities. In *Asteroids* (T. Gehrels, Ed.), pp. 528–557. Univ. of Arizona Press, Tucson.

Davis, D. R., E. V. Ryan, and P. Farinella 1994. Asteroid collisional evolution: Results from current scaling algorithms. *Planet. Space Sci.* **42**, 599–610.

Duncan, M. J. 1994. Orbital stability and the structure of the Solar System. In *Circumstellar Dust Disks and Planet Formation* (R. Ferlet and A. Vidal-Madjar, Eds.), pp. 245–255. Editions Frontières, Gifsur Yvette.

Duncan, M. J., and H. F. Levison 1997. A scattered comet disk and the origin of Jupiter family comets. *Science* **276**, 1670–1672.

Duncan, M. J., H. F. Levison, and S. M. Budd 1995. The dynamical structure of the Kuiper belt. *Astron. J.* **110**, 3073–3081.

Everhart, E. 1985. An efficient integrator that uses Gauss–Radau spacings. In *Dynamics of Comets: Their Origin and Evolution* (A. Carusi and G. B. Valsecchi, Eds.), pp. 185–202. Reidel, Dordrecht.

Fernández, J. A., and W. H. Ip 1996. Orbital expansions and the resonant trapping during the late accretion stages of the outer planets. *Planet. Space Sci.* **44**, 431–439.

Gladman, B., J. J. Kavelaars, P. Nicholson, T. Loredo, and J. A Burns 1998. Pencil-beam surveys for faint trans-neptunian objects. *Astron. J.* **116**, 2042–1054.

Gomes, R. S. 1997. Dynamical effects of planetary migration on the primordial asteroid belt *Astron. J.* **114**, 396–401.

Gradie, J. C., and E. F. Tedesco 1982. Compositional structure of the asteroid belt. *Science* **216**, 1405–1407.

Hahn, J., and R. Malhotra 1999. Orbital evolution of planets embedded in a planetesimal disk. *Astron. J.*, in press.

Heppenheimer, T. A. 1980. Secular resonances and the origin of the eccentricities of Mars and the asteroids. *Icarus* **41**, 76–88.

Holman, M. J., and N. W. Murray 1996. Chaos in high-order mean motion resonances in the outer asteroid belt. *Astron. J.* **112**, 3, 1278–1293.

Ida, S., and J. Makino 1992. *N*-body simulation of gravitational interaction between planetesimals and a protoplanet. I. Velocity distribution of planetesimals. *Icarus* **96**, 107–120.

Ip, W. H. 1987. Gravitational stirring of the asteroid belt by Jupiter zone bodies. *Gerland. Beitr. Geophys.* **96**, 44–51.

Jewitt, D. C., J. X. Luu, and J. Chen 1996. The Mauna Kea—Cerro Tololo (MKCT) Kuiper belt and Centaur survey. *Astron. J.* **112**, 1225–1238.

Jewitt, D. C., J. X. Luu, and C. Trujillo 1998. Large Kuiper belt objects: The Mauna Kea 8k CCD Survey. *Astron. J.* **115**, 2125–2135.

Kenyon, S. J., and J. X. Luu 1998. Accretion in the early Kuiper belt. I. Coagulation and velocity evolution. *Astron. J.* **115**, 2136–2160.

Knežević, Z., A. Milani, P. Farinella, Ch. Froeschlé, and C. Froeschlé 1991. Secular resonances from 2 to 50 AU. *Icarus* **93**, 316–330.

Lecar, M., and F. Franklin 1997. The solar nebula, secular resonances, gas drag, and the asteroid belt. *Icarus* **129**, 134–146.

Lemaitre, A., and P. Dubru 1991. Secular resonances in the primitive solar nebula. *Celest. Mech. Dynam. Astron.* **52**, 57–78.

Levison, H. F., and M. Duncan 1994. The long-term dynamical behavior of short-period comets. *Icarus* **108**, 18–36.

Levison, H. F., and M. Duncan 1997. From the Kuiper belt to Jupiter-family comets: The spatial distribution of ecliptic comets. *Icarus* **127**, 13–32.

Levison, H. F., E. M. Shoemaker, and C. S. Shoemaker 1997a. The dispersal of the Trojan swarm. *Nature* **385**, 42–45.

Levison, H. F., S. A. Stern, and M. J. Duncan 1997b. The role of a massive primordial Kuiper belt on its current dynamical structure. *Icarus*, submitted for publication.

Liou, J. C., and R. Malhotra 1997. Depletion of the outer asteroid belt. *Science* **275**, 375–377.

Lissauer, J. J., and G. R. Stewart 1993. Growth of planets from planetesimals. In *Protostars and Planets III* (E. H. Levy and J. I. Lunine, Eds.), pp. 1061–1088. University of Arizona Press, Tucson.

Malhotra, R. 1993. Orbital resonances in the solar nebula—Strengths and weaknesses. *Icarus* **106**, 264.

Malhotra, R. 1995. The origin of Pluto's orbit: Implications for the Solar System beyond Neptune. *Astron. J.* **110**, 420–429.

Morbidelli, A. 1997. Chaotic diffusion and the origin of comets from the 2/3 resonance in the Kuiper belt. *Icarus* **127**, 1–12.

Morbidelli, A. 1998. The structure of the Kuiper belt and the origin of the Jupiter-family comets. In *Solar System Formation and Evolution* (D. Lazzaro *et al.*, Eds.), pp. 83–105. Astron. Soc. Pacific, Conference Series.

Morbidelli, A., and G. B. Valsecchi 1997. Neptune scattered planetesimals could have sculpted the primordial Edgeworth–Kuiper belt. *Icarus* **128**, 464–468.

Morbidelli, A., F. Thomas, and M. Moons 1995. The resonant structure of the Kuiper belt and the dynamics of the first five trans-neptunian objects. *Icarus* **118**, 322–340.

Öpik, E. J. 1976. *Interplanetary Encounters*. Elsevier, New York.

Parisi, M. G., and A. Brunini 1996. Dynamical consequences of Uranus' great collision. In *Chaos in Gravitational N-Body Systems* (J. C. Muzzio, S. Ferraz-Mello, and J. Henrard, Eds.), pp. 291–296. Kluwer Academic, Dordrecht/Norwell.

Pollack, J. B., O. Hubickyj, P. Bodenheimer, J. J. Lissauer, M. Podolak, and Y. Greenzweig 1996. Formation of the giant planets by concurrent accretion of solids and gas. *Icarus* **124**, 62–85.

Ruzmaikina, T. V., V. S. Safronov, and S. J. Weidenschilling 1989. Radial mixing of material in the asteroidal zone. In *Asteroids II* (R. P. Binzel, T. Gehrels, and M. S. Matthews, Eds.), pp. 681–700. Univ. of Arizona Press, Tucson.

Safronov, V. S. 1966. Sizes of the largest bodies falling onto the planets during their formation. *Sov. Astron.* **9**, 987–991.

Safronov, V. S. 1979. On the origin of asteroids. In *Asteroids* (T. Gehrels, Ed.), pp. 975–993. Univ. of Arizona Press, Tucson.

Stern, S. A. 1991. On the number of planets in the outer Solar System: Evidence of a substantial population of 1000-km bodies. *Icarus* **90**, 271–281.

Stern, S. A. 1996. The collisional environment and accumulation timescale constraints in the primordial massive Kuiper disk. *Astron. J.* **112**, 1203–1211.

Stern, S. A., and J. E. Colwell 1997. Collisional erosion in the primordial Edgeworth–Kuiper belt and the generation of the 30–50 AU Kuiper gap. *Astrophys. J.* **490**, 879–882.

Stern, S. A., D. Durda, and R. Canup 1999. *Lunar Planet. Sci. Conf. 31st*, submitted.

Stoer, J., and R. Bulirsch 1980. In *Introduction to Numerical Analysis*. Springer-Verlag, New York.

Tegler, S. C., and W. Romanishin 1998. Two distinct populations of Kuiper-belt objects. *Nature* **392**, 49–51.

Valsecchi, G. B., and A. Manara 1997. Dynamics of comets in the outer planetary region. II. Enhanced planetary masses and orbital evolutionary paths. *Astron. Astrophys.* **323**, 986–998.

Ward, W. R. 1980. Scanning secular resonances: A cosmogonical broom? *Proc. Lunar Planet. Sci. Conf. 11th*, pp. 1199–1201.

Ward, W. R., G. Colombo, and F. A. Franklin 1976. Secular resonance, solar spin down, and the orbit of Mercury. *Icarus* **28**, 441–452.

Weidenschilling, S. J. 1977. The deistribution of mass in the planetary system and solar nebula. *Astrophys. Space Sci.* **51**, 153–158.

Weissman, P. R., and H. F. Levison 1996. The population of the trans-neptunian region: The Pluto–Charon environment. In *Pluto and Charon* (S. A. Stern and D. J. Tholen, Eds.), pp. 559–604. Univ. of Arizona Press, Tucson.

Wetherill, G. W. 1989. Origin of the asteroid belt. In *Asteroids II* (R. P. Binzel, T. Gehrels, and M. S. Matthews, Eds.), pp. 661–680. Univ. of Arizona Press, Tucson.

Wetherill, G. W. 1992. An alternative model for the formation of the asteroids. *Icarus* **100**, 307–325.

Wetherill, G. W., and J. E. Chambers 1997. Numerical integration study of primordial clearing of the asteroid belt. *Proc. Lunar Planet. Sci. Conf. 28th*, p. 1547.

Wisdom, J. 1980. The resonance overlap criterion and the onset of stochastic behavior in the restricted three-body problem. *Astron. J.* **85**, 1122–1133.